



Bachelor Thesis

# Variability of the Isotopic and Hydrochemical Composition of Lake Bol'shoe Toko, SE Yakutia, Russia

Presented to the

**Institute of Earth and Environmental Sciences**

**University of Potsdam**

In partial fulfillment of the

requirement for the degree

**Bachelor of Science in Geosciences**

by

**Till Hainbach**

Supervised by

**Dr. Hanno Meyer**

**apl. Prof. Dr. Bernhard Diekmann**

**Dr. Boris Biskaborn**

Potsdam, November 2016



# Table of Contents

|   |           |
|---|-----------|
| Table of Figures .....  | III       |
| List of Tables .....  | III       |
| List of Abbreviations.....  | IV        |
| Abstract .....  | V         |
| Zusammenfassung.....  | VI        |
| <b>1 Introduction.....</b>  | <b>1</b>  |
| <b>2 Study Area .....</b>   | <b>3</b>  |
| 2.1 Limnological setting .....  | 3         |
| 2.2 Geological setting .....  | 5         |
| 2.3 Climatic setting .....  | 5         |
| <b>3 Materials &amp; Methods.....</b>   | <b>7</b>  |
| 3.1 Stable isotope geochemistry in water analysis .....                         | 7         |
| 3.1.1 Fundamentals of stable isotope geochemistry.....                          | 7         |
| 3.1.2 Fractionation of stable isotopes .....                                    | 8         |
| 3.1.3 Effects on stable isotopes within the hydrological cycle .....            | 11        |
| 3.1.4 Stable isotope measurements .....   | 12        |
| 3.2 Analytical methods for hydrochemical water analysis .....                   | 13        |
| 3.2.1 ICP OES .....   | 13        |
| 3.2.2 Analysis of bicarbonate in water .....                                    | 14        |
| 3.2.3 Ion exchange chromatography.....  | 15        |
| 3.2.4 pH-value measurements in water .....                                      | 15        |
| 3.2.5 Measurement of dissolved oxygen (DO) .....                                | 16        |
| 3.3 Fieldwork.....  | 16        |
| <b>4 Results.....</b>   | <b>17</b> |
| 4.1 Variability of the isotopic composition at Lake Bol'shoe Toko .....         | 17        |
| 4.1.1 Spatial variation of the isotopic composition at Bol'shoe Toko .....      | 17        |
| 4.1.2 Isotope-depth profiles from Lake Bol'shoe Toko and its surroundings ..... | 20        |
| 4.2 Hydrochemical composition of Bol'shoe Toko .....                            | 23        |
| <b>5 Discussion.....</b>  | <b>25</b> |
| 5.1 Water and precipitation sources for Lake Bol'shoe Toko .....                | 25        |

|     |  |    |
|-----|--|----|
| 5.2 | The isotopic signal of Lake Bol'shoe Toko and its spatial variations ..... | 28 |
| 5.3 | Isotope-depth relationship at Lake Bolshoe Toko .....                      | 30 |
| 5.4 | Discussion of the hydrochemical composition .....                          | 32 |
| 5.5 | Lake Bol'shoe Toko in regional comparison .....                            | 34 |
| 6   | Conclusions.....   | 36 |
| 7   | Outlook .....  | 37 |
|     | References .....   | 38 |
|     | Appendix.....  | i  |
|     | Acknowledgments.....   | v  |

## Table of Figures

|   |    |
|---|----|
| Figure 1: Topographic map of Central and Eastern Siberia.....   | 3  |
| Figure 2: Map of Lake Bol'shoe Toko and its limnological and geological setting.....  | 4  |
| Figure 3: Climate diagram for Toko RS (after Walter and Lieth (1960)).....  | 6  |
| Figure 4: Fractionation processes of stable water isotopes and their effects on a meteoric water line .....   | 10 |
| Figure 5: Scheme of a mass spectrometer .....   | 12 |
| Figure 6: Scheme of the Perkin Elmer Optima 8300 ICP OES .....  | 14 |
| Figure 7: $\delta^{18}\text{O}$ - $\delta\text{D}$ -plot for all water samples and GNIP data from Yakutsk .....   | 18 |
| Figure 8: Isotopic composition of surface water samples from Lake Bol'shoe Toko. ....   | 18 |
| Figure 9: Isotope-depth and temperature-depth profiles at PG2208 .....  | 20 |
| Figure 10: Isotope-depth and temperature-depth profile at PG2122 "Lagoon", SE of Lake Bol'shoe Toko .....   | 22 |
| Figure 11: Isotope-depth and temperature-depth profile for site PG2131 "Bania Lake" .....   | 22 |
| Figure 12: Piper (1944) Plot for all water samples of different sample sites .....  | 23 |
| Figure 13: Annual mean $\delta\text{D}$ and $\delta^{18}\text{O}$ in precipitation patterns (Isoscapes) for North Asia....  | 26 |
| Figure 14: HYSPLIT back trajectory frequencies prior to both 6-day precipitation events in August 2012 (06-08.08.2012 (A), 17.-22.08.2012 (B)) and to the precipitation event 1-3 April 2013 (C)..... | 27 |
| Figure 15: Isotope-depth profiles for both water (red) and lake ice (turquoise) at site PG2208, Lake Bol'shoe Toko.....   | 30 |

## List of Tables

|   |     |
|---|-----|
| Table 1: Terrestrial abundances of stable oxygen and hydrogen isotopes .....  | 7   |
| Table 2: mean isotopic composition of snow, lake ice, and water samples from the respective lake basin or water profile. .... | 19  |
| Table 3: Isotopic composition of snow and ice samples taken at Lake Bol'shoe Toko. ....                                       | i   |
| Table 4: Isotope and hydrochemistry data for all water samples taken in March 2013 .....                                      | ii  |
| Table 5: Hydrochemistry data for all water samples taken in March 2013 .....  | iii |
| Table 6: Isotope data for water samples taken in August 2012 .....  | iv  |

## List of Abbreviations

|          |  |
|----------|--|
| a.s.l.   | above sea level                                      |
| BP       | before Present (before 1950)                         |
| BT       | Bol'shoe Toko  |
| d-excess | Deuterium excess                                     |
| DIC      | Dissolved Inorganic Carbon                           |
| GMWL     | Global Meteoric Water Line                           |
| GNIP     | Global Network of Isotopes in Precipitation          |
| HDW2     | Mixed standard water from the Potsdam region         |
| HTM      | Holocene thermal maximum                             |
| IC       | Ion Exchange Chromatograph                           |
| ICP OES  | Inductive-Coupled Plasma Optic Emission Spectroscopy |
| IRMS     | Isotope Ratio Mass Spectrometer                      |
| KARA     | Kara Sea Water (standard)                            |
| LMWL     | Local Meteoric Water Line                            |
| NGT      | North Greenland Traverse (standard)                  |
| OIPC     | Online Isotopes in Precipitation Calculator          |
| Precip.  | Precipitation  |
| SEZ      | Severnaja Zemlja water (standard)                    |
| Temp.    | Temperature  |

## Abstract

High latitudes of the northern hemisphere are most vulnerable to climate warming, but impose a great threat due to positive feedback mechanism, such as enhanced greenhouse-gas emissions as a consequence of permafrost degradation. In the Russian Far-East, however, predictions are biased due to large research gaps. Hence, further investigations on recent climate patterns are essential to achieve better estimates for future environmental change in boreal Russia.

In this context, open surface waters, such as lakes, provide valuable information about precipitation sources and seasonal variability in remote areas of Siberia. Stable water isotopes are good climate proxies due to temperature dependent fractionation process. Therefore, water, ice and snow samples were taken at a lake (Bol'shoe Toko, BT) in a little explored region in Southern Yakutia in 2012 and 2013. Analyses of the isotopic and hydrochemical composition were carried out to obtain a profound knowledge of the present hydrological regime.

Water isotope analyses at Lake Bol'shoe Toko show only little variations spatially as well as throughout the water column. The mean isotopic composition of  $\delta^{18}\text{O} = -18.2 \pm 0.2 \text{ ‰}$  and  $\delta\text{D} = -137 \pm 1 \text{ ‰}$  show no significant seasonal variations comparing a summer and winter profile. There is no indication for evaporation enrichment found at Lake Bol'shoe Toko. However, fractionation alters the isotopic composition of surface waters during ice-cover formation. In contrast, water of the side lake "Bania Lake" (East of Lake Bol'shoe Toko) is enriched in heavy isotopes, indicating evaporative enrichment during summer, whereas water in a lagoon (South-East of Lake Bol'shoe Toko) have a slightly lower isotopic composition. Waters from all three lakes are of Ca-Mg-HCO<sub>3</sub>-type and show unpolluted freshwater conditions with low conductivity. However, nitrate concentration in the lagoon are at a critical level for algae growth.

All in all, Lake Bol'shoe Toko is an oligotrophic, well-mixed, open through-flow lake system with no pronounced seasonal variability. Changes in isotopic and hydrochemical composition of the lagoon and Bania Lake are directly link to the geological and geomorphological setting of Lake Bol'shoe Toko, as precipitation and substantially surface run-off control the hydrological regime.

## Zusammenfassung

Die hohen Breiten der nördlichen Hemisphäre sind vom Klimawandel am meisten betroffen, aber stellen aufgrund von positiven Rückkopplungsmechanismen auch eine große Gefahr dar, wie zum Beispiel erhöhte Treibhausgasemission aufgrund von Permafrostdegradation. Jedoch sind Vorhersagen für das fernöstliche Russland durch große Forschungslücken verzerrt. Um zukünftige Umweltveränderungen im borealen Russland besser vorhersagen zu können, benötigt es weiterer Studien über die rezenten Klimamuster. In diesem Zusammenhang können offene Oberflächengewässer, wie Seen, wertvolle Information über Niederschlagsquellen und saisonale Schwankungen in den abgelegenen Gebieten Sibiriens liefern. Wegen ihrer temperaturabhängigen Fraktionierung sind stabile Wasserisotopen gute Klimaproxies. Daher wurden 2012 und 2013 Wasser-, Eis- und Schneeproben aus einem See (Bol'shoe Toko, BT) in einer wenig erforschten Region in Süd-Yakutien entnommen. Analysen der Isotopen- und hydrochemischen Zusammensetzung wurde durchgeführt, um so ein tiefgründiges Verständnis der rezenten Hydrologie zu erhalten. Die Isotopenanalysen zeigen nur geringe Schwankung, sowohl in der Fläche als auch in der Wassersäule. Die durchschnittliche Isotopenzusammensetzung von  $\delta^{18}\text{O} = -18.2 \pm 0.2 \text{ ‰}$  und  $\delta\text{D} = -137 \pm 1 \text{ ‰}$  zeigte keine signifikanten saisonalen Veränderungen zwischen Sommer- und Winterprofil. Es gab keine Anzeichen für evaporativen Anreicherungen im Bol'shoe Toko See. Jedoch verändern Fraktionierungsprozesse die Isotopenzusammensetzung von Oberflächenwässer während der Ausbildung der Seeeissschicht. Im Gegensatz dazu waren Wasserproben aus dem Nebensee „Bania See“ (im Osten des Bol'shoe Toko Sees) mit schwereren Isotopen angereichert, was auf evaporative Anreicherung in den Summermonaten hindeutet. Indessen hatten Wasserproben aus der Lagune im Südosten des Bol'shoe Toko Sees eine leicht leichtere Isotopenzusammensetzung. Gewässerproben der drei untersuchten Seen waren vom Ca-Mg-HCO<sub>3</sub>-Type und zeigten nicht verschmutzte Frischwasserbedingungen mit geringer Leitfähigkeit. Jedoch waren die Nitratkonzentrationen in der Lagune auf einem kritischen Niveau für das Algenwachstum.

Alles im allem ist der Bol'shoe Toko See ein oligotropher, gut gemischter, offener Durchfluss-See mit keiner ausgeprägten saisonalen Schwankung. Veränderungen in der Isotopen- und hydrochemischen Zusammensetzung der Lagune und des Bania Sees sind direkt verknüpft mit dem geologischen und geomorphologischen Hintergrund des Bol'shoe Toko Sees, da Niederschlag und vor allem Oberflächenablauf die Hydrologie beeinflussen.

# 1 Introduction

High latitudes of the northern hemisphere are most vulnerable to climate warming (Zhang et al., 2000, ACIA, 2004). In boreal Russia, models predict an increase of annual mean surface temperature of up to + 11°C (Giorgetta, 2012). Increasing surface temperatures enhanced permafrost thawing and snow cover melting, thus leading to further emission of greenhouse gases (e.g. methane) from soils and albedo reduction, respectively. Therefore, ongoing warming of high latitudes results in further global warming due to positive feedback mechanisms (Schuur and Abbott, 2011). Accurate estimates on environmental impact, however, are biased due to large research gaps in understanding the sub-recent paleoclimate in the Russian Far-East (Miller et al., 2010).

Here, stable water isotopes can provide valuable information to improve the understanding of the recent climate system. Since the mid 1950s, stable water isotopes have been used to investigate the hydrological cycle and climate patterns (Craig, 1961a, Dansgaard, 1964, Rozanski et al., 1993, Araguás-Araguás et al., 1998). Nonetheless, most of these studies are based on long term observation of the isotopic composition in precipitation.

Such observations, however, are insufficient for large parts of the remote areas of Siberia, but information can be derived from open surface waters. First studies of stable isotope behavior in lake water hydrology were carried out by Craig and Gordon (1965) and subsequently improved (e.g. Dincer, 1968, Zuber, 1983, Gat, 1995). With the beginning of the new millennia, isotopic studies were conducted investigating the linkage between surface waters and precipitation on a broader regional scale (Gibson et al., 2002, Ichiyanagi et al., 2003, Mayr et al., 2007, Gibson and Reid, 2010).

Additionally, hydrochemical analysis has been widely used to obtain key information on the hydrology controls of lake systems, e.g. in identifying source water and different drainage regions as well as acquiring knowledge about the geogenic background and limitation of aquatic biota (e.g. Parnachev and Degermendzhy, 2002, Rogora et al., 2003). Furthermore, information about water hydrochemistry is essential for assessing possible anthropogenic influences on limnological ecosystems (e.g. Reimann et al., 1999).

Consequently, the combination of stable isotope and hydrochemical analyses leads to a profound knowledge about the hydrological regime of surface water systems. This includes information such as recent lake temperature, isotopic composition, precipitation and water

sources and their respective seasonal changes as well as possible changes of water lake level and input signals over time.

On this basis, multi-proxy studies of lake sediments cores can provide high resolution and continuous information on environmental and climatic change (Leng and Barker, 2006), hence, allowing paleoclimate reconstruction from a terrestrial perspective.

At the Alfred-Wegener Institute Helmholtz Centre for Polar and Marine Research (AWI), bioindicators, sedimentological and geochemical data of lake sediment cores from different lake systems through Central and Eastern Siberia were investigated (e.g. Biskaborn et al., 2012, Biskaborn et al., 2013, Nazarova et al., 2013, Schleusner et al., 2015) within the SibLake Program ([Eastern Siberian Lakes \(SibLake Programme\)](#)). Two transects of north-south and west-east orientation aim to distinguish different climatic influences on paleoenvironmental changes, e. g. the temporal delay of the Holocene thermal maximum (HTM) from north to south Yakutia (Biskaborn et al., 2016).

In this context, the investigation of Lake Bol'shoe Toko aims to extend the understanding of recent climate variability in southward direction. Previously conducted research indicated a pristine natural environment, though Konstantinov (2000) reported possible anthropogenic influences due to enhanced coal mining activity in southern Yakutia adjacent to Lake Bol'shoe Toko.

Several water samples and sediment cores were retrieved during a joint expedition of AWI and the North-Eastern Federal University of Yakutsk (NEFU) in 2013. This thesis is part of a series of theses on Lake Bol'shoe Toko that are based on samples taken during the March 2013 expedition. First assessments on sedimentology (Löffler, 2016) and taxonomy of chironomids (Weniger, 2016) and diatoms (Dreßler, 2016) have already been carried out. A thesis on oxygen isotopes in sub surface diatoms is in progress (Wollenweber, 2017, in prep.). In this context, the presented study aims to provide import background information about the hydrological regime at Lake Bol'shoe Toko. For this, the isotopic and hydrochemical composition of the lake water, as well as in snow and ice samples were analysed and interpreted regarding the local geomorphological and geological setting and its contribution to lake water variability. The findings are then discussed within the regional context.

## 2 Study Area

The Republic of Sakha or Yakutia covers most of the central part of Siberia. It extends from the Gulf of Khatanga eastward over the northeast Siberian Lowland to the Kolyma Gulf. From there its border trends south-westwards to the Aldan Upland, crossing the Northeast Siberian Highlands. The Southern border is marked by the southern edge of the Aldan Upland and the Tokinsky-Stanvoi mountain ranges which also form the frontier of the Nerjungri coal deposits. The western frontier of the republic of Sakha trends from the Khatanga Gulf southward to the Baikalian ranges.



Figure 1: Topographic map of Central and Eastern Siberia.

### 2.1 Limnological setting

The Lake Bol'shoe Toko is located at 56°15'N, 130°30'E in South-East Yakutia at the border of the Republic of Sakha and the Region Khabarovsk. It is 300 km inland to the east from the Sea of Okhotsk and lies at 903 m a.s.l. The lake is 15 km in length and 7 km in width and covers a surface of approximately 82.6 km<sup>2</sup> (Konstantinov, 2000). It has a maximum water depth of 80 m at the western margin of the lake, whereas the northern margin is relatively shallow (20-10 m deep).

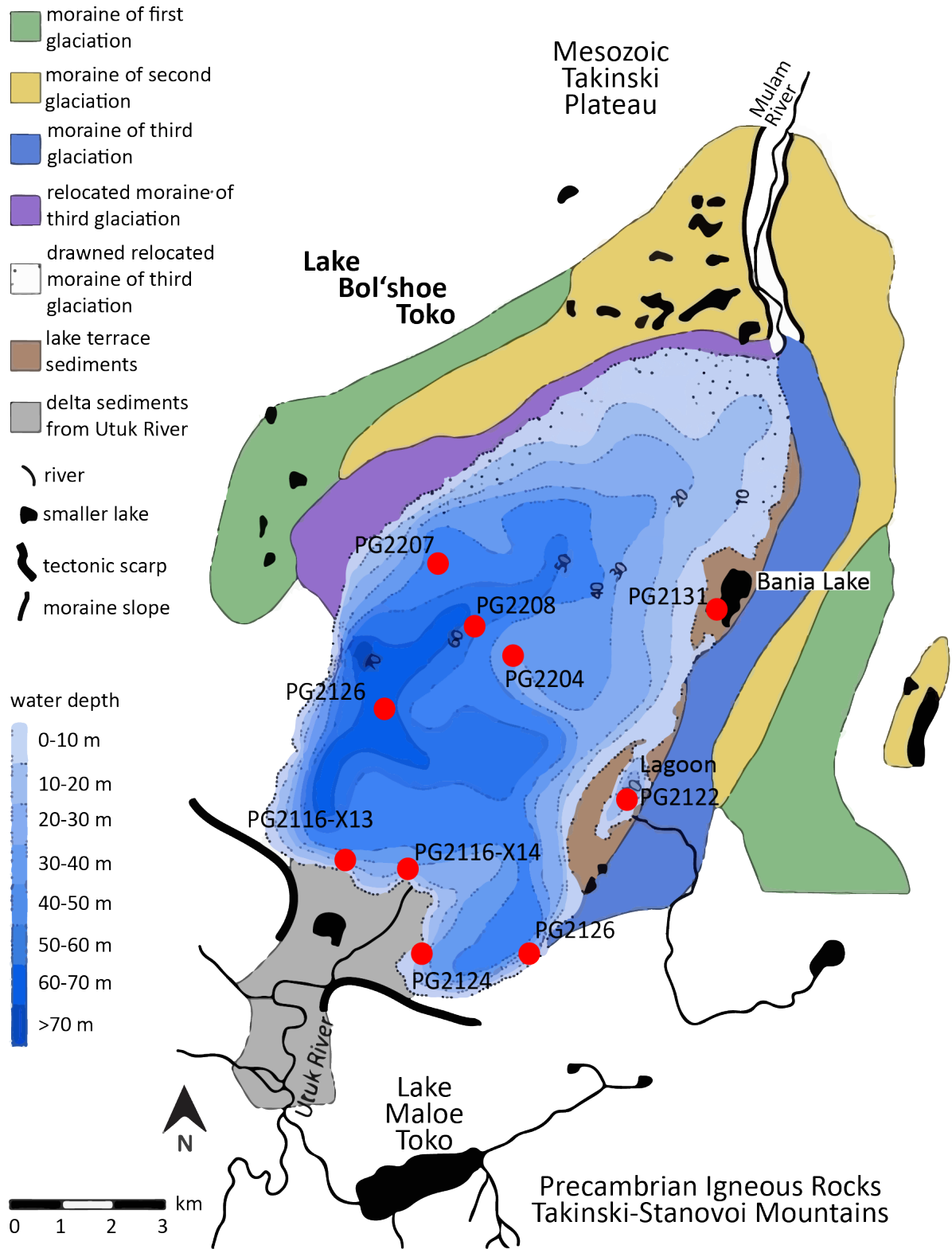


Figure 2: Map of Lake Bol'shoe Toko and its limnological and geological setting. Red points indicate water sample sites. Original map was measured at 1 km grid and therefore contains uncertainties in water depths. Compiled by B. Biskaborn combining the data from Konstantinov (2000) and Kornilov (1962), both Russian literature.

The Utuk river brings water from the southern igneous catchment, additionally fed by the runoff of Lake Maloe Toko (a smaller lake of tectonic origin approximately 3 km south of the Lake Bol'shoe Toko) and forms deltaic sediments. A second unnamed tributary river runs into a shallower (< 20 m) lagoon at the eastern part of Lake Bol'shoe Toko. The lagoon is nearly separated from the Bol'shoe Toko basin and has just a narrow and shallow connection of less than 80 m in width. Lake Bol'shoe Toko has one main outflow called Mulam river which runs northward along the southeastern border of Yakutia into Uzur, Aldan and ultimately into Lena River (Konstantinov, 2000).

## **2.2 Geological setting**

The Lake Bol'shoe Toko is of tectonic and glacial origin. It lies in a depression formed by two NW-trending right-lateral strike-slip faults (Imaeva et al., 2009) reshaped by at least three glacial sub-periods. The basin is dammed in the north by the moraines of these glaciations (Kornilov, 1962).

Along the southern margin of the lake runs the South Tokin thrust fault, one of the most active faults in the region (earthquakes recorded in 1977 and 1979), where highly mafic granulites and other high-pressure metamorphic rocks of the Tokin Stanovoi orogen are thrust over coal-rich Jurassic and Cretaceous deposits. The potential coal resources were estimated to 40 billion tons in 1981 being the most promising coal basin of the Baikal-Amur-Mainline (Jensen et al., 1983). The geodynamic activity is also shown in its high heat flow (Imaeva et al., 2009).

## **2.3 Climatic setting**

The Republic of Sakha covers three climatic zones. The coast of the Laptev Sea lies within the arctic tundra zone. Further South, where the tundra vegetation gives way to the vast taiga forest, a small strip of subarctic climate regime is attached. The South of Yakutia lies within the climate regime of temperate continental climate (Shahgedanova, 2002). The Siberian anticyclone, a regional high pressure system predominantly active between November and March, is mainly responsible for very cold winters, with clear sky and low precipitation. In Summer, due to the landlocked position of Central Siberia, maximum temperatures often exceed +30°C. As the atmosphere is depleted in moisture and central Siberia itself is shielded by several orogens, precipitation ranges between 200-600 mm per year. Yakutsk's long weather record reports a mean annual precipitation of about 250 mm/year and a mean annual

temperature of  $-10.2^{\circ}\text{C}$  with a for continental sites characteristic high temperature amplitude (January mean, July mean) of 55 K (Gavrilova, 1993).

The closest weather station to the study site is “Toko RS”. It is located 10 km northeast of lake Bol’shoe Toko and has a lower mean annual temperature ( $-11.2^{\circ}\text{C}$ ) but higher precipitation (276-579 mm/year) than Yakutsk (Konstantinov, 2000). Most of the precipitation (50%) occurs in the Summer months (223 mm in June-August) as rainfall whereas precipitation from November to March does not exceed 30 mm/month (see Figure 3). Winter precipitation (December to February) just amounts to 7 % of the annual precipitation. Most of the year, mean surface air temperatures are below the freezing point (October-April) but exceed  $0^{\circ}\text{C}$  in early to late summer (May to September).

At Lake Bol’shoe Toko, Konstantinov (2000) reports lower temperature measurements as a result of cold water discharge from the mountains and high volume of ice during winter.

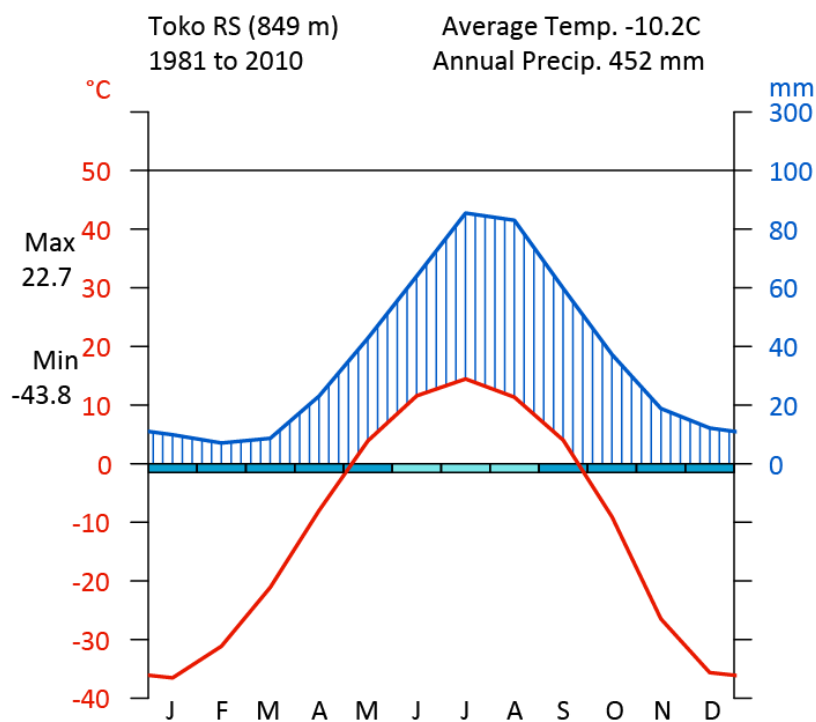


Figure 3: Climate diagram for Toko RS (after Walter and Lieth (1960)). Climate data record taken from NOAA. Dark blue bars indicate probable freezing; light blue bars indicate possible freezing. The water saturation is given throughout the year.

### 3 Materials & Methods

#### 3.1 Stable isotope geochemistry in water analysis

##### 3.1.1 Fundamentals of stable isotope geochemistry

Isotopes are defined as nuclides which have the same number of protons but differ in the number of neutrons. Hence, these nuclides belong to the same element but are differentiated by their atomic weight defined by the sum of protons and neutrons. Depending on the number of neutrons an isotope can be stable or unstable. Unstable (radioactive) isotopes can spontaneously disintegrate into other isotopes (of the same or another element) by different modes of decay whilst stable isotopes do not decay within detection limits (Clark and Fritz, 1997, Hoefs, 2015). About 300 stable isotopes exist worldwide (Hoefs, 2015), this research however focuses on with the stable hydrogen (H), and oxygen (O) isotopes only, which are also called stable water isotopes.

There are two stable hydrogen isotopes,  $^1\text{H}$  and  $^2\text{H}$  (the latter also called deuterium, D), whereas oxygen has three stable isotopes ( $^{16}\text{O}$ ,  $^{17}\text{O}$ ,  $^{18}\text{O}$ ), which differ in their atomic mass and their terrestrial abundances (see Table 1).

As different ratios of hydrogen and oxygen isotopes exist, water molecules may have different molecular weights. These differences in mass lead to different reaction rates which then cause isotopic fractionation i.e. during water phase transitions (Clark and Fritz, 1997).

Table 1: Terrestrial abundances of stable oxygen and hydrogen isotopes (after Kloss, 2008).

| element  | isotope         | atomic mass | natural abundance [%] |
|----------|-----------------|-------------|-----------------------|
| hydrogen | $^1\text{H}$    | 1           | 99.985                |
|          | D               | 2           | 0.015                 |
| oxygen   | $^{16}\text{O}$ | 16          | 99.76                 |
|          | $^{17}\text{O}$ | 17          | 0.04                  |
|          | $^{18}\text{O}$ | 18          | 0.2                   |

As differences in isotopic compositions of various waters are relatively small, an isotopic ratio of a sample is expressed as the relative permil deviation from a standard isotope ratio. This deviation is given as the so called  $\delta$ -value given in per mil (‰).

In general, the  $\delta$ -value is calculated as:

$$\text{Equation 1: } \delta_{\text{sample}} = \left\{ \frac{R_{\text{sample}}}{R_{\text{standard}}} - 1 \right\} * 1000 \text{ ‰}$$

For water isotopes, Craig (1961b) defined the Standard Mean Ocean Water (SMOW) as a reference. According to the assumption that the oceans, as uniform and very large reservoirs, are the basis of the meteorological cycle, its  $\delta$ -value was defined as 0 ‰. When SMOW standard, calibrated from an old US-reference water, was exhausted, the International Atomic Energy Agency (IAEA) prepared a new standard water whose isotopic composition nearly matches the SMOW. This standard, called VSMOW (Vienna Standard Mean Ocean Water), is the internationally accepted reference for  $^{18}\text{O}$  and  $^2\text{H}$  in waters (Clark and Fritz, 1997).

Consequently, Equation 1 is adapted to:

$$\text{Equation 2: } \delta^{18}\text{O}_{\text{sample}} = \left\{ \frac{\left( \frac{^{18}\text{O}}{^{16}\text{O}} \right)_{\text{sample}}}{\left( \frac{^{18}\text{O}}{^{16}\text{O}} \right)_{\text{VSMOW}}} - 1 \right\} * 1000 \text{ ‰}$$

$$\text{Equation 3: } \delta D_{\text{sample}} = \left\{ \frac{\left( \frac{\text{D}}{\text{H}} \right)_{\text{sample}}}{\left( \frac{\text{D}}{\text{H}} \right)_{\text{VSMOW}}} - 1 \right\} * 1000 \text{ ‰}$$

for oxygen and hydrogen, respectively.

### 3.1.2 Fractionation of stable isotopes

In each thermodynamic reaction, differences in reaction rates cause a disproportionate concentration of one isotope over the other. This enrichment of one isotope over the other is called isotopic fractionation and expressed by the fractionation factor  $\alpha$  (Clark and Fritz, 1997). The factor is defined as the isotope ratio in a compound A divided by the isotope ratio in compound B (Hoefs, 2015).

$$\text{Equation 4: } \alpha_{A-B} = \frac{R_A}{R_B}$$

In terms of water, fractionation occurs mainly while it changes its state (e.g. water to vapor). Water molecules consisting of lighter isotopes have weaker intermolecular bonds than those formed of heavier isotopes and are therefore easier to disintegrate. Hence, whilst a water phase change, lighter waters are preferentially turned into a state of aggregation in which

they are less bonded. So, phases with weak intermolecular bonding (e.g. the gaseous phase) get enriched in lighter isotopes and depleted in heavy isotopes (Clark and Fritz, 1997).

Depending on the physicochemical reaction, the isotope partitioning occurs under either equilibrium or kinetic conditions both of which are fundamental in the hydrological cycle. Due to wind shear, sea surface temperature, salinity and, most importantly, relative humidity, evaporation of sea water imparts kinetic conditions on the fractionation. This is because transport of water-vapor from the sea surface to the atmosphere and vice versa is only equal in both directions under high humidity conditions (near to 100 % relative humidity). The global average humidity, however, is 85 %. As lighter water molecules are preferentially turned into the vapor phase and their diffusivity is higher than that of heavier isotopes, the atmospheric water-vapor is depleted in heavy isotopes relative to the ocean basin. With temperature increase, the fractionation factor  $\alpha$  decreases, because lighter and heavier isotopes get evaporated more equally (Hoefs, 2015).

In contrast, condensation occurs under equilibrium conditions as initial rainout/droplet formation requires a relative humidity of 100%. According to the concept described above, heavier water molecules (enriched in  $^{18}\text{O}$  and D) favorably condense into water droplets. Therefore, atmospheric moisture gets further depleted in heavy isotopes with each precipitation event as the rain is enriched in D and  $^{18}\text{O}$  isotopes relative to the vapor. This ongoing depletion in heavy isotopes is called Rayleigh distillation (Clark and Fritz, 1997), which is also described as the rainout effect in the hydrological cycle.

Although the processes of the hydrological cycle are rather complex, Craig (1961a) found a linear correlation between  $^{18}\text{O}$  and D in global fresh waters, described as global meteoric water line (GMWL) with the following equation:

$$\text{Equation 5: GMWL: } \delta D = 8 \cdot \delta^{18}\text{O} + 10 \text{ ‰ [SMOW]}$$

Three decades later, Rozanski et al. (1993) refined this relationship based on global precipitation data from the Global Network for Isotopes in Precipitation (GNIP):

$$\text{Equation 6: } \delta D = 8 (\pm 0.06) \cdot \delta^{18}\text{O} + 10.35 (\pm 0.65) \text{ ‰ [SMOW]}$$

The slope of 8 in Equation 5 and Equation 6 is caused by equilibrium condensation in the cloud and represents the relationship between the fractionation factors of oxygen and hydrogen.

Re-evaporation, as a kinetic process, leads to a slope lower than 8 and depends on humidity (Figure 1). The interception of the GMWL with the  $\delta D$  at 10 ‰ reflects the global average relative humidity of 85 % (Hoefs, 2015). Dansgaard (1964) first characterized the deuterium excess (d-excess) in global precipitation as:

$$\text{Equation 7:} \quad d_{\text{excess}} = \delta D - 8 \cdot \delta^{18}\text{O}$$

The d-excess reflects mainly the humidity conditions at the moisture source. It increases with decreasing relative humidity (Merlivat and Jouzel, 1979, Clark and Fritz, 1997).

On a more local scale, both the slope, the intercept and the d-excess can vary significantly. These variations are then expressed in local meteoric water lines (LMWL) with respective slopes and intercepts.

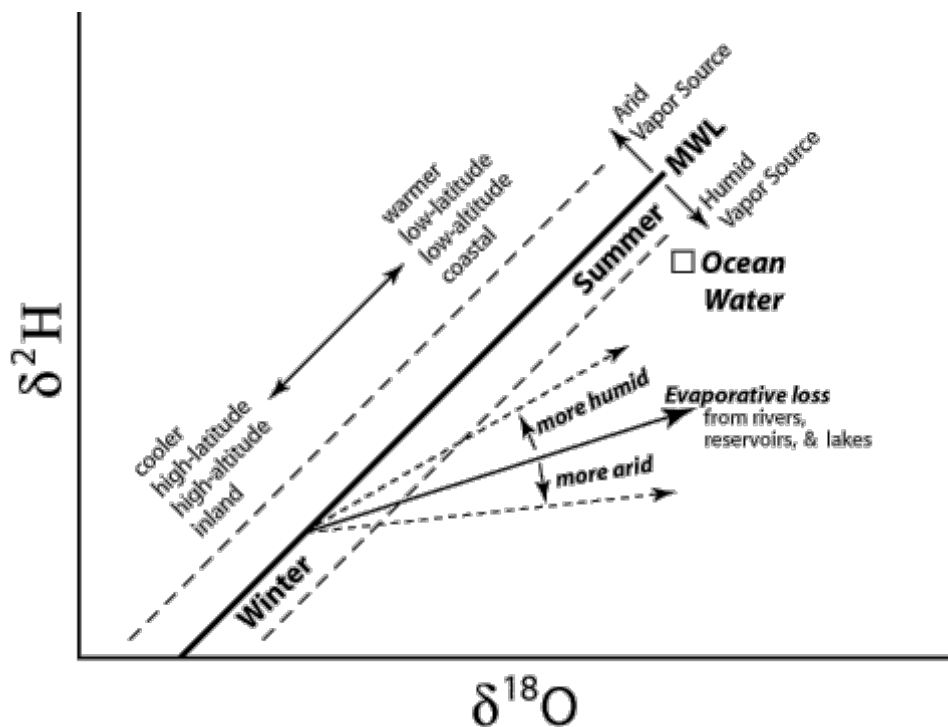


Figure 4: Fractionation processes of stable water isotopes and their effects on a meteoric water line (SAHRA, 2005).

In general, a cooler region has more negative (lower) isotopic composition, whereas warmer regions are associated with higher  $\delta$ -values (see Figure 4). This can be explained by the aforementioned temperature dependency of isotope fraction at the moisture source. Since vapor pressure of HDO/H<sub>2</sub>O on one hand and H<sub>2</sub><sup>18</sup>O and H<sub>2</sub><sup>16</sup>O on the other differs slightly (heavier waters have lower vapor pressure), changes in relative humidity during evaporation

alter the fractionation of oxygen and hydrogen isotopes by different magnitudes. As a result, such changes are reflected in the d-excess. Therefore, more arid moisture sources plot above the GMWL. Correspondingly, humid moisture sources plot below the GMWL (Figure 4). If evaporation occurs within open water bodies, the residual water gets enriched in heavy isotopes. As shown, fractionation during kinetic processes is of higher magnitude for oxygen isotopes than for hydrogen isotopes. Consequently, the residual water is shifted below the GMWL. When such waters contribute moisture to precipitation, the slope differs from that of the GMWL (Clark and Fritz, 1997).

### 3.1.3 Effects on stable isotopes within the hydrological cycle

In the hydrological cycle, the initial moisture is depleted in heavy isotopes with respect to the oceans. During rain, heavier isotopes are preferentially precipitated leading to a depletion in heavy isotopes relative to initial moisture. This process is progressively enhanced while the moisture is transported landwards, due to Rayleigh distillation. Hence with increasing distance to the moisture origin, the  $\delta$ -values of the vapor mass become more and more negative. This is described as the **continental effect**, although large water bodies within the continents may diminish the effect (Clark and Fritz, 1997).

Dansgaard (1964) showed that a decrease in temperature leads to more negative  $\delta$ -values. As vapor masses, generally originated in low latitudes, are transported polewards (higher latitudes) to cooler regions, they become depleted in heavy isotopes. This is described as the **latitude effect** (Figure 4).

The temperature dependency of water isotope fractionation also leads to seasonal variations in the  $\delta$ -values. Especially at continental stations with high annual Temperature amplitude, summer precipitation is enriched in heavy isotopes compared to the winter precipitation. This is known as the **seasonality effect** (Figure 4).

When vapor masses are uplifted by orography they cool down under adiabatic conditions. Hence with increasing altitude the precipitation has gradually decreasing  $\delta$ -values. This kind of Rayleigh distillation of water vapor to the top of a mountain is called the **altitude effect** (Clark and Fritz, 1997).

The amount effect describes changes in the isotopic composition due to evaporation during a precipitation event (Dansgaard, 1964). While humidity is low during light rain, it is high for heavy rain. As described above, humidity influences the fractionation during evaporation

leading to an alteration of the isotopic signal. For light rain, the raindrops are enriched in heavy isotopes, and for heavy rain, signal is changed towards more negative  $\delta$ -values respectively.

### 3.1.4 Stable isotope measurements

The stable isotopic composition of water samples can be analytically determined by various methods, with isotope ratio mass spectrometry (IRMS) being still the most prevalent. The principle is the separation of atoms and molecules based on their masses. For that, a magnetic field is applied on a beam of charged molecules, bending it into its spectrum of masses (Clark and Fritz, 1997).

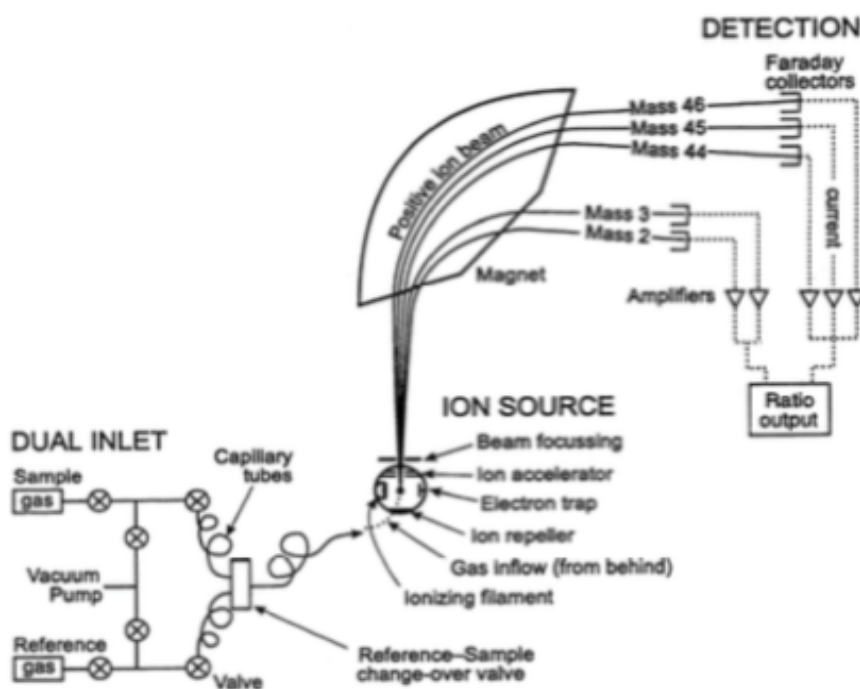


Figure 5: Scheme of a mass spectrometer (after Clark and Fritz (1997)).

A gas mass spectrometer consists of an inlet system, an ion source, the flight tube with installed electro-magnet and a detection unit (see Figure 5). Within the ion source, a heated tungsten-coated iridium filament ionizes a  $H_2$  or  $CO_2$  gas stream entering from the inlet system. Subsequently, the positively charged gas molecules are accelerated by a voltage gradient and focused into the flight tube where the ion beam is deflected by an electromagnetic field. Due to specific mass-to-charge ratios of the isotopes, the gradient of deflection varies and thus the beam is split. At the end of the flight tube, several faraday cup collectors are attached, allowing for simultaneous measurements for each ion current. The signal is enhanced and expressed as mass-to-charge ratios (Clark and Fritz, 1997).

At the AWI Potsdam, a Finnigan-MAT Delta S IRMS with dual inlet system was used. At the front end, two equilibration units (MS Analysetechnik, Berlin) with a total capacity of 48 samples are attached. The equilibration units are kept in a water-shaking bath at  $18^{\circ}\text{C} \pm 0.01$  to prevent condensation. A 3-5 ml aliquot of water sample is filled into a glass bottle and a platinum-coated stick is added as a catalyst. The bottles are screwed onto the equilibration unit and evacuated before gas is applied. For  $\delta\text{D}$ -determination, hydrogen gas ( $\text{H}_2$ ) is used and equilibrated for 180 minutes. After the  $\delta\text{D}$ -measurement,  $\text{CO}_2$  is applied and equilibrated 400 minutes for  $\delta^{18}\text{O}$ -analysis. Consequently, both the  $\delta\text{D}$  and  $\delta^{18}\text{O}$ -values are measured on the exact same sample aliquot (Meyer et al., 2000).

Subsequent to equilibration, the gas is transferred into the inlet system. A cooling trap (ethanol-dry ice mixture) at  $-78^{\circ}\text{C}$  prevents water vapor from entering the IRMS. Both units are equipped with the laboratory standard NGT-1 on the first position which serves as the reference gas during the analysis. Each sample is measured 10 times.

The MS output is processed with ISODAT (version 5.2) to express the  $\delta$ -values as ‰-differences relative to the international standard VSMOW (Meyer et al., 2000).

If the internal error ( $1\sigma$ ) exceeds  $\pm 0.8$  ‰ for  $\delta\text{D}$  and  $\pm 0.1$  ‰ for  $\delta^{18}\text{O}$ , respectively, the measurement is repeated. Additionally, to ensure quality control, six to eight sample bottles per unit are filled with various standard waters. The standards are selected to match the expected isotopic composition of the water samples (Meyer et al., 2000). For Siberia, the standard waters NGT, KARA, SEZ and HDW2 are used.

## **3.2 Analytical methods for hydrochemical water analysis**

### **3.2.1 ICP OES**

To analyze the cation composition of a water sample, the ICP OES has been the favored method since the mid 80's. The technique is based upon two units: the ICP (inductive-coupled plasma) and the OES (optical emission spectrometry). In the ICP unit, a sample is ionized and excited electrons are produced which emit electromagnetic radiation (light) at characteristic wavelengths. The created spectrum of emitted light is then analyzed in the OES unit (Figure 6). The ICP unit consists of 3 quartz tubes (called "torch") surrounded by an electromagnetic coil. When the torch is turned on, a high frequency electromagnetic field is generated by the coil. An Argon gas stream is ignited by a discharge arc of a Tesla unit initiating the ionization

process. As a result, a plasma consisting of positively charged Argon ions and free electrons is generated. At the end of the torch the plasma is cut off by a stream of compressed air.

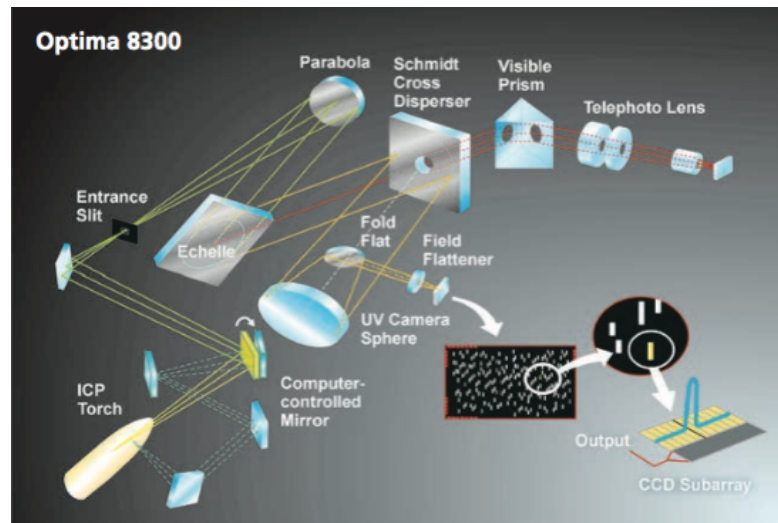


Figure 6: Scheme of the Perkin Elmer Optima 8300 ICP OES (taken from Perkin Elmer supplement material).

Using a peristaltic pump, a sample is sucked into an analytical nebulizer turning the sample into mist which then is directly introduced into the plasma. The high energy of the plasma (up to 10000 K) breaks down the molecules into their respective atoms which then are ionized. Within the ions electrons are excited to higher energy levels (orbitals) emitting electromagnetic waves when they jump back to their orbital of origin. These characteristic wavelengths create a spectrum of light which is analyzed by OES unit.

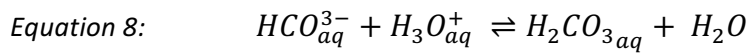
In the OES unit the emitted light is first focused using toroidal mirrors and then diffracted using an echelle grating. Secondly, the light is split into a visible and a UV light fraction using a Schmidt-cross disperser. Both light fractions are then analyzed by a Segmented-array Charge-coupled device (SCD). For a better detection at varying element concentrations two viewing perspectives are used: the axial and the radial view (Nölte, 2002).

At the Alfred-Wegener-Institute the Perkin Elmer Optima 8300 ICP OES is used.

### 3.2.2 Analysis of bicarbonate in water

To measure the amount of bicarbonate in water, a sample is titrated with hydrochloric acid until it reaches a pH-value of 4.3. The amount of acid used is then calculated into the concentration of bicarbonate in water.

When acid is added to a (bi-)carbonate buffered water, the bicarbonate (or carbonate ions for alkaline waters) react with dissolved hydronium ions forming carbon acid.



Therefore, the pH-value of the water does not change proportionally to the acid input. At a pH-value of 4.3 the fraction of bicarbonate ion to dissolved inorganic carbon (DIC) is < 1%.

Derived from Equation 8, the start concentration (before the addition of acid) of bicarbonate can be calculated as:

$$\text{Equation 9: } \quad c_{\text{HCO}^{3-}} = c_{\text{acid}} \cdot \frac{V_{\text{acid}}}{V_{\text{sample}}} \cdot M_{\text{HCO}^{3-}} \cdot 1000 \text{ [mg/l]}$$

Bicarbonate concentrations were measured using a Metrohm 794 Basic Titrino.

### 3.2.3 Ion exchange chromatography

To analyze the anion composition of water samples, a IC Dionex DX 320 ion exchange chromatograph was used.

An ion exchange chromatograph (IC) consists of a mobile phase, a stationary phase and a detector unit. The mobile phase is an eluent into which the sample (analyte) is injected. The stationary phase consists out of a polymer matrix with countercharged ions. When the mobile phase is pumped into the separation column, the stationary phase retains the ions of the analyte based on coulombic (ionic) interactions. Depending on the strength of the binding with the stationary phase, different ions in the analyte pass the separation column at different speeds and hence get separated. At the end of the column a detector unit (e.g. conductivity meter) measures the concentrations of the ions. In modern IC a suppressor unit suppresses the conductivity signal of the eluent.

### 3.2.4 pH-value measurements in water

For determination of the pH-value of a water sample, a pH-meter is used which is a set of a pH-sensitive electrode (normally a glass electrode), a reference electrode and a temperature element. The glass electrode is filled with a buffered solution. When getting in contact with a

solution, water ions tend to accumulate around silicate groups resulting in a potential (voltage). This potential is proportional to the pH-value of the solution. The reference electrode maintains a given potential at any temperature. As a result, a signal current (in millivolt [mV]) is measured from which the pH-value of the sample can be derived. For pH-determination a WTW Multi 340i probe was used.

### **3.2.5 Measurement of dissolved oxygen (DO)**

For measurements of dissolved oxygen in water, an optical sensor (WTW Multi 340i probe) was used. In the sensor a luminophor is excited by light and its decay is measured by a photodiode. When getting into contact with oxygen (O<sub>2</sub>) the luminophor passes its excitation energy to the oxygen molecule which results in a characteristic alteration of the decay.

## **3.3 Fieldwork**

During late March and early April 2013, 7 surface water samples of Lake Bol'shoe Toko as well as 3 water profiles from the center of Lake Bol'shoe Toko, the lagoon and the smaller side Bania Lake were collected using a 1.5 l UWITEC water sampler with integrated temperature measurement. The upper 10 m were sampled at 0, 2, 5 and 10 m water depth. For waters at greater depth, a resolution of one sample per 10 m was chosen, to account for any possible variation within the deeper water layers. After sampling, water samples were filled into previously rinsed 250 ml PET bottles

Additionally, one ice core of 82 cm depth was retrieved from the ice cover of Lake Bol'shoe Toko and split at 10 cm resolution. Furthermore, Snow samples were collected from the snow cover of Lake Bol'shoe Toko. One precipitation event on 2 April 2013 was sampled. Both, ice and snow samples were melted in the field at room temperature.

At the field camp laboratory, conductivity, pH-value and oxygen saturation was determined using a WTW Multi 340i probe. Before each measurement session, the probe was calibrated according to information provided by WTW. All measurements were carried out at room temperature ( $\approx 20^{\circ}\text{C}$ ).

Samples for anion and cation analyses were filtrated using a 0.45  $\mu\text{m}$  cellulose acetate filter. Cation samples were additionally acidified with ultrapure nitric acid (65 % HNO<sub>3</sub>) to pH  $\approx 2$ , for conservation.

## 4 Results

### 4.1 Variability of the isotopic composition at Lake Bol'shoe Toko

To describe the variability of the isotopic composition at Lake Bol'shoe Toko (in figures abbreviated as "BT"), the data is subdivided into a spatial set of surface water samples taken from the lake and a set of water samples taken vertically along the water column at different sites. Additionally, one ice core of 80 cm depth at sample site PG2208, as well as two ice samples in the south of Lake Bol'shoe Toko near the mouth of Utuk River, where the ice cover was unexpectedly thin ( $< 3.5$  cm), were taken and analyzed for their isotopic composition to investigate possible fractionation processes during ice cover season. Furthermore, snow samples (from the ice cover on the lake and one precipitation event during the expedition) were collected. In total, 6 snow samples, one precipitation event, 10 ice samples, 7 surface water samples and 4 water profiles with a total of 37 water samples were analyzed.

#### 4.1.1 Spatial variation of the isotopic composition at Bol'shoe Toko

Generally, all surface water samples, taken from the main Lake Bol'shoe Toko, are within the range of  $\delta^{18}\text{O}_{\text{surface}} = -18.6 \pm 0.1$  ‰ ( $-139 \pm 1$  ‰ in  $\delta\text{D}$ ). However, samples taken at the south of the lake near the mouth of the Utuk river have a slightly heavier isotopic composition ( $\delta^{18}\text{O} = -18.4$  ‰) than samples taken from the lake center (Figure 8), whereas water samples taken near the western shore are isotopically slightly lighter ( $\delta^{18}\text{O} = -18.7$  ‰). Unfortunately, a clear statement regarding the northern part of Lake Bol'shoe Toko cannot be made due to missing sample data.

Comparing all samples in a  $\delta^{18}\text{O}$ - $\delta\text{D}$ -plot (Figure 7), it is evident that water samples taken from the lagoon and Lake Bol'shoe Toko are situated close to the GMWL, whereas waters of the side lake "Bania Lake" are shifted towards heavier isotope values and lower d-excess onto the LMWL of Yakutsk ( $\delta\text{D} = 7.57 * \delta^{18}\text{O} - 6.86$  (Kloss, 2008)). The mean isotopic composition of water samples taken in March along the water column at Lake Bol'shoe Toko ( $\delta^{18}\text{O}_{\text{PG2208}} = -18.2 \pm 0.2$  ‰) is slightly heavier than the mean of surface samples ( $\delta^{18}\text{O}_{\text{surface}} = -18.6 \pm 0.1$  ‰), resulting in  $\delta^{18}\text{O}_{\text{March}} = -18.4 \pm 0.2$  ‰ for all samples taken at Lake Bol'shoe Toko. Water samples taken in August 2012, show higher variation (see Figure 7) and have a slightly lighter mean isotopic composition ( $\delta^{18}\text{O}_{\text{August}} = -18.2 \pm 0.2$  ‰) than the March mean but similar to the mean of PG2208.

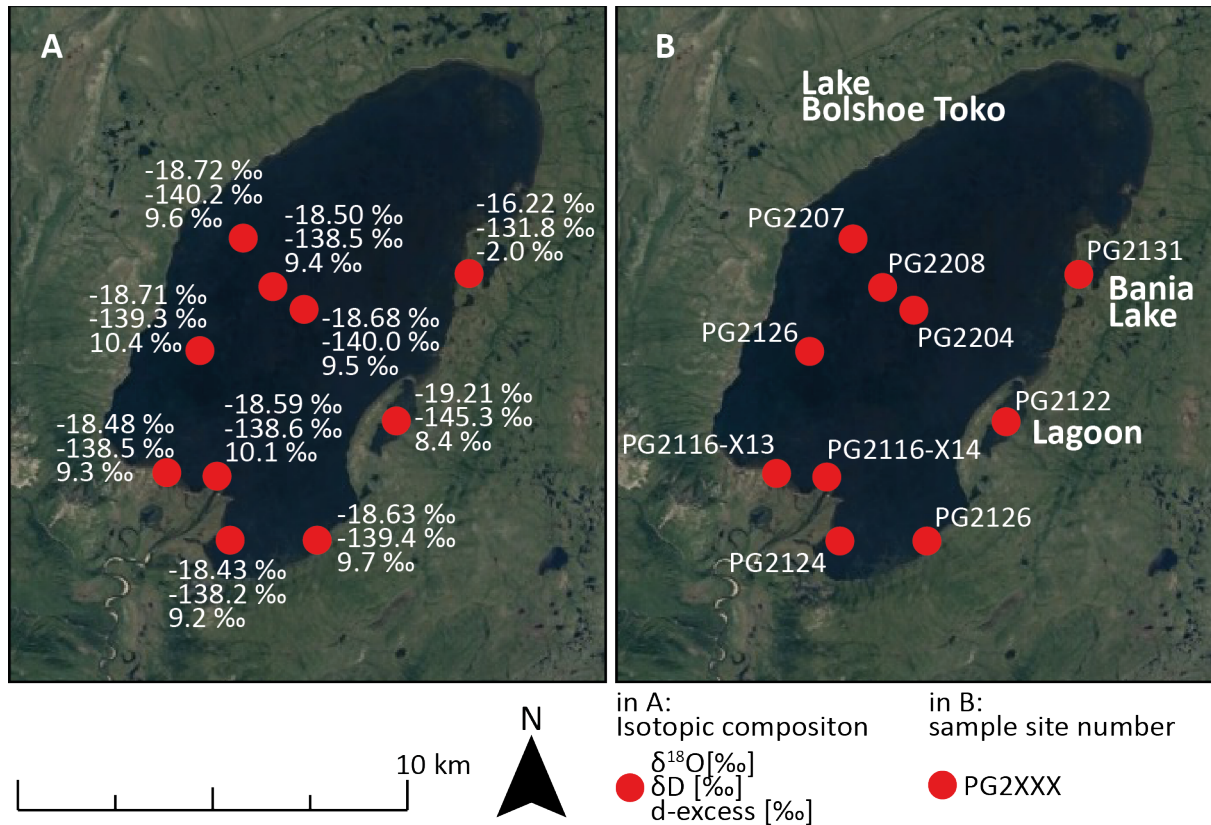


Figure 8: Isotopic composition of surface water samples from Lake Bol'shoe Toko.

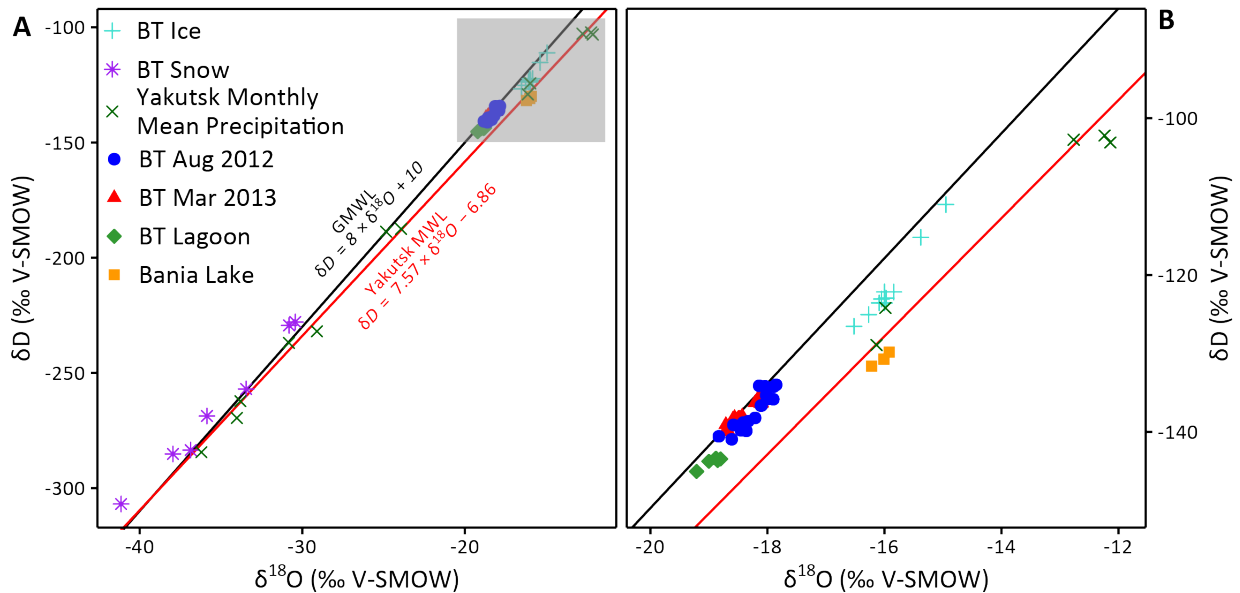


Figure 7:  $\delta^{18}\text{O}$ - $\delta\text{D}$ -plot for all water samples and GNIP data from Yakutsk. Grey shaded area in plot A is enhanced in plot B. Generally, water samples from Bol'shoe Toko (August samples in blue, March samples in red) and Lagoon (green) as well as snow samples plot well on the GMWL, whereas water samples taken from the Bania Lake are situated on the LMWL of Yakutsk.

In contrast, the water samples of the lagoon are shifted towards lighter isotopic composition by 0.5 ‰ ( $\delta^{18}\text{O}_{\text{lagoon}} = -18.9 \pm 0.2 \text{ ‰}$ ). The highest isotopic composition in water was measured at Bania Lake ( $\delta^{18}\text{O}_{\text{Bania}} = -16.1 \pm 0.2 \text{ ‰}$ ) showing clearly an enrichment in heavy isotopes compared to Lake Bol'shoe Toko and the lagoon.

The isotopic composition of snow samples is depleted in heavy isotopes and range from -30.8 ‰ in  $\delta^{18}\text{O}$  (-227.9 ‰ in  $\delta\text{D}$ ) to -41.1 ‰ in  $\delta^{18}\text{O}$  (-306.9 ‰ in  $\delta\text{D}$ ). With exception of two samples, all snow samples are located above the GMWL (Figure 7). Vice versa, lake ice samples are enriched in heavy isotopes (-16.1 ‰ in  $\delta^{18}\text{O}$  and -123.8 ‰ in  $\delta\text{D}$ ), with two outliers at -15.38 ‰ in  $\delta^{18}\text{O}$  (-115.3 ‰ in  $\delta\text{D}$ ) and -14.95 ‰ in  $\delta^{18}\text{O}$  (-111.1 ‰ in  $\delta\text{D}$ , see Figure 7) and plot below the GMWL.

*Table 2: mean isotopic composition of snow, lake ice, and water samples from the respective lake basin or water profile.*

| Site  | $\delta^{18}\text{O}$ [‰]<br>vs. VSMOW | standard<br>deviation | $\delta\text{D}$ [‰]<br>vs. VSMOW | standard<br>deviation | d-excess [‰]<br>vs. VSMOW | standard<br>deviation |
|---|--|-----------------------|-----------------------------------|-----------------------|---------------------------|-----------------------|
| Mean Isotopic composition of snow and lake ice samples at Bol'shoe Toko |  |                       |                                   |                       |                           |                       |
| snow  | -35.2                                  | 3.9                   | -266                              | 30                    | 16                        | 4                     |
| lake ice  | -15.9                                  | 0.4                   | -122                              | 5                     | 6                         | 1                     |
| Mean Isotopic composition of water samples from Lake Bol'shoe Toko      |  |                       |                                   |                       |                           |                       |
| BT Surface  | -18.6                                  | 0.1                   | -139                              | 1                     | 10                        | 1                     |
| BT March 2013   | -18.4                                  | 0.2                   | -138                              | 2                     | 9                         | 1                     |
| BT August 2012  | -18.2                                  | 0.3                   | -137                              | 2                     | 8                         | 1                     |
| PG2208  | -18.2                                  | 0.2                   | -137                              | 1                     | 9                         | 1                     |
| Mean Isotopic composition of the lagoon and Bania Lake                  |  |                       |                                   |                       |                           |                       |
| lagoon  | -18.9                                  | 0.2                   | -144                              | 1                     | 7                         | 1                     |
| Bania   | -16.1                                  | 0.2                   | -131                              | 1                     | -3                        | 0                     |

## 4.1.2 Isotope-depth profiles from Lake Bol'shoe Toko and its surroundings

### 4.1.2.1 Site PG2208, Lake Bol'shoe Toko

Two water profiles were taken from Lake Bolshoe Toko. One (red signature in Figure 9) was taken in March 2013 during the winter campaign at the approximate center of Lake Bol'shoe Toko (sample site PG2208) with a water depth of 68 m. The other water profile (blue signature in Figure 9) was taken in August 2012 by L. Pestryakova at a sample site near the western shoreline with a water depth of only 37 m.

The isotopic composition of water samples taken in March 2013 at PG2208 from Lake Bolshoe Toko show little variability throughout the profile (see Figure 9). In contrast the  $\delta$ -values from samples taken in August 2012 show much larger variations. For March the  $\delta^{18}\text{O}$  value stabilizes from 10 m downward at around  $-18.2\text{‰}$  and the  $\delta\text{D}$ -value at  $-136\text{‰}$ , while the ratios above 10 m upward to the ice cover show a trend to lighter isotope values, shifted by  $-0.5\text{‰}$  in  $\delta^{18}\text{O}$

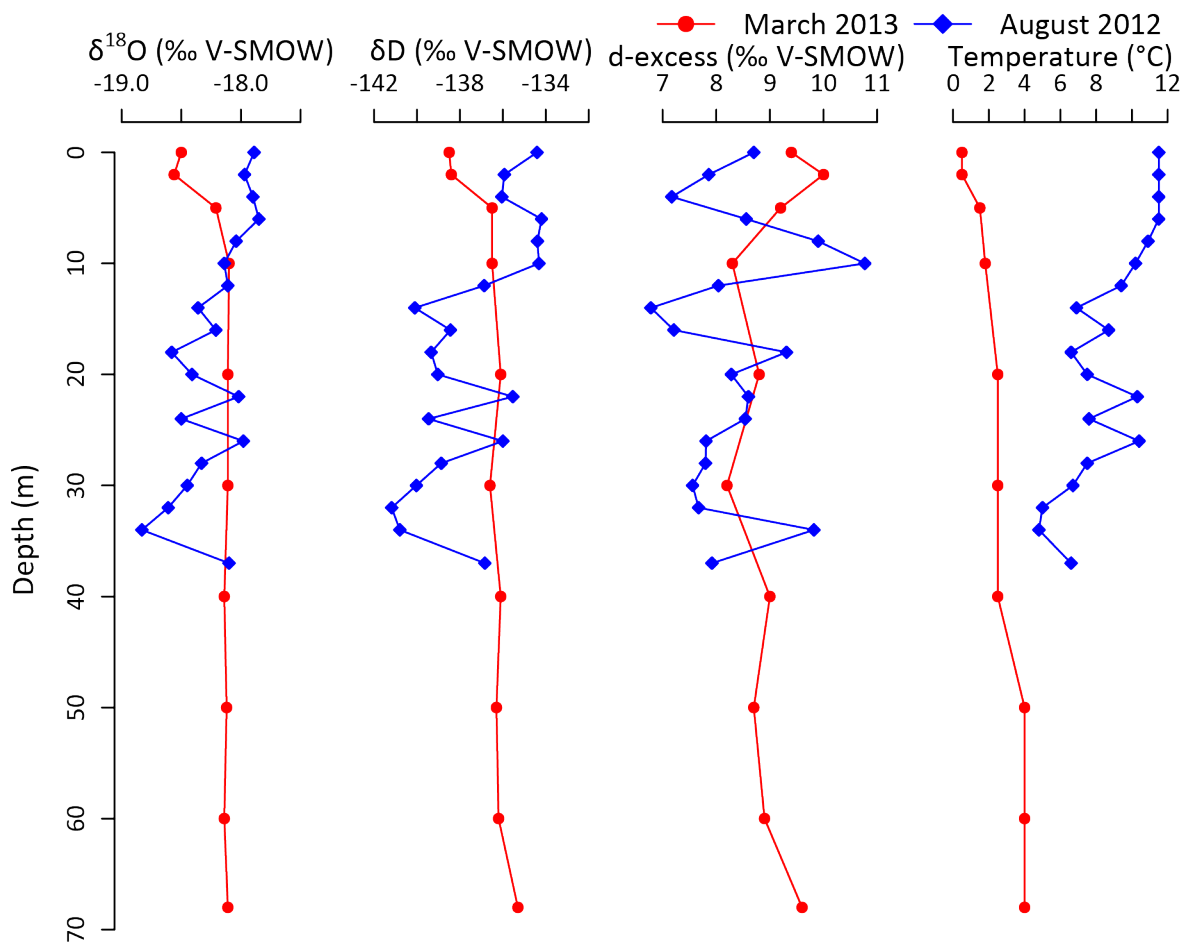


Figure 9: Isotope-depth and temperature-depth profiles at PG2208 for oxygen and hydrogen as well as d-excess of measured samples for March 2013 (red) and August 2012 (blue, samples provided by L. Pestryakova, L.A; NEFU Yakutsk)

and -2 ‰ in  $\delta D$ , respectively. Furthermore, there is a slight shift towards less negative values at the lower end at a depth of 68 m. In this profile, the d-excess shows a similar but mirror-inverted picture. For waters >10 m in depth the d-excess ranges between 8-9 ‰ except at 68 m, whereas the uppermost meters show slightly higher d-excess values of 9-10 ‰. In March, the mean isotopic composition of Lake Bol'shoe Toko is  $-18.2 \pm 0.2$  ‰ in  $\delta^{18}O$ ,  $-137 \pm 1$  in  $\delta D$  and  $9 \pm 1$  ‰ in d-excess.

The August data shows a more complex relationship. In general, the isotopic composition for the uppermost 10 m display higher values between -18.2 ‰ and -17.7 ‰ for  $\delta^{18}O$  and -136 ‰ to -134 ‰ for  $\delta D$ , respectively, as compared to the March data. Beneath, the values decrease to lighter isotopic composition until 20 m below water surface. Between 20 m and 30 m they oscillate around  $-18.3 \pm 0.5$  ‰ for  $\delta^{18}O$  and  $-137 \pm 2$  ‰ for  $\delta D$ . Downwards, the isotopic composition shifts to lighter ratios, with an increase at 36 m (above sediment surface). Generally, the d-excess values show an almost similar development, varying between 6 ‰ and 11 ‰. The August data has a mean isotopic composition of  $-18.2 \pm 0.3$  ‰ in  $\delta^{18}O$ ,  $-137 \pm 2$  ‰ in  $\delta D$  and  $8 \pm 1$  ‰ in d-excess.

Comparing both profiles, it is evident that a first main shift appears at a depth of 10 m, whereas two more shifts are seen in the profile for August. Furthermore, both profiles have the same mean isotopic composition, although their isotope-depth relationships differ strongly.

#### **4.1.2.2 Site PG2122, "Lagoon"**

The water profile of PG2122, taken in March 2013, located in the lagoon at the SE of the lake shows a similar isotopic trend compared to PG2208, although the values are isotopically lighter by 0.5 ‰ in  $\delta^{18}O$  and 8 ‰ in  $\delta D$ , respectively (Figure 10). As at PG2208, near-surface samples  $\delta^{18}O$  and  $\delta D$  are depleted in heavier isotopes but as the basin is much shallower (18 m water depth) the effect is limited to the upper 3-5 m. In contrast, the d-excess decreases from  $\approx 8$  ‰ to  $\approx 7$  ‰. The mean isotopic composition for the lagoon is  $-18.9 \pm 0.2$  ‰ in  $\delta^{18}O$  and  $-114 \pm 1$  ‰ in  $\delta D$ , respectively.

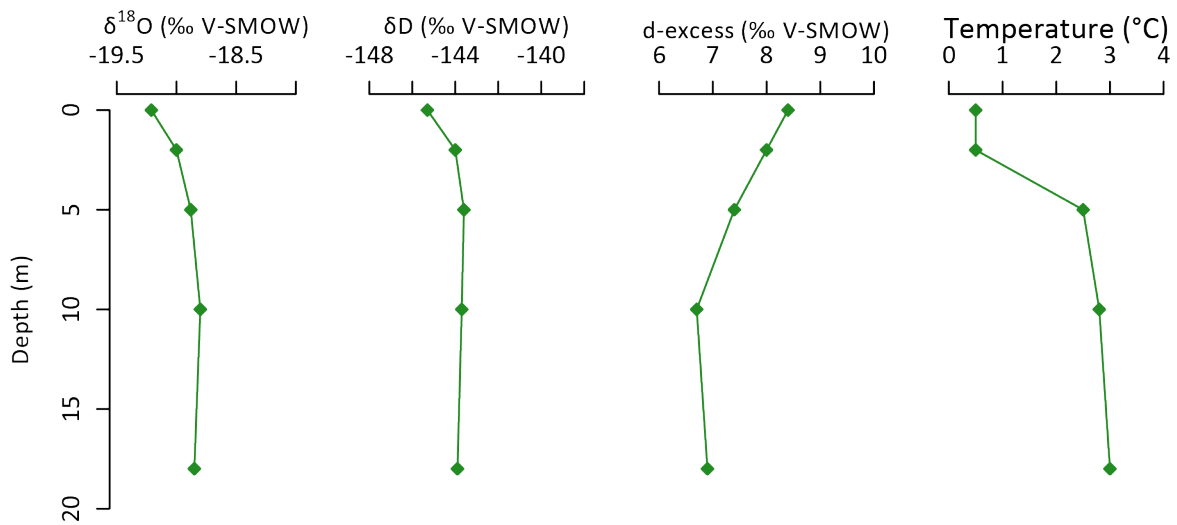


Figure 10: Isotope-depth and temperature-depth profile at PG2122 "Lagoon", SE of Lake Bol'shoe Toko. Generally, similar trends compared to the main basin are observed but lighter isotopic composition.

#### 4.1.2.3 Isotope-depth profile at site PG2131, "Bania Lake"

A shallower profile of the side lake "Bania Lake" (6 m in water depth) is enriched in heavy isotopes compared to the water profiles of Lake Bol'shoe Toko and the lagoon. Its isotopic composition varies slightly between -16.0 ‰ at 3 m and -16.3 ‰ at the surface for  $\delta^{18}\text{O}$ , and from -132 ‰ at 3 m to -130 ‰ at the surface in  $\delta\text{D}$ , accordingly (Figure 11). The d-excess values show significant differences compared to PG2122 and PG2208.

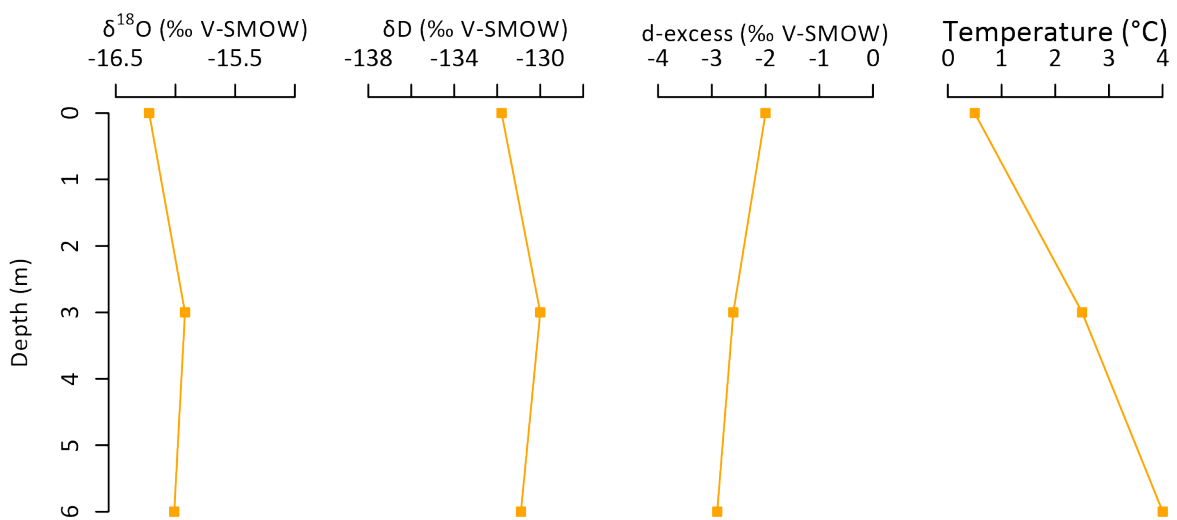


Figure 11: Isotope-depth and temperature-depth profile for site PG2131 "Bania Lake". Samples taken in March 2013

They vary between -3 ‰ at the bottom (6 m) and -2 ‰ at the surface, differing by 10 ‰ compared to Lake Bol’shoe Toko. The mean  $\delta^{18}\text{O}_{\text{Bania}}$  =  $-16.1 \pm 0.2$  ‰ and  $\delta\text{D}_{\text{Bania}}$  =  $-131 \pm 1$  ‰.

### 4.2 Hydrochemical composition of Bol’shoe Toko

For all three basins, the sampled waters are well saturated in O<sub>2</sub> (92-120 %) with a pH-value from neutral to slightly acid (6.4 – 7.2). The electrical conductivity is very low for all waters, though the lagoon shows a 1.5-2 times higher conductivity (64.5  $\mu\text{S}/\text{cm}$ ) than the Lake Bol’shoe-Toko (29.1 – 42.9  $\mu\text{S}/\text{cm}$ , 35.0  $\mu\text{S}/\text{cm}$  in average) and the Bania Lake (40.4  $\mu\text{S}/\text{cm}$ ). All basins were show thermal stratification, with four identified layers for the Bol’shoe Toko main basin (with thermoclines at around 5, 20 and 50 m water depth), two layers for the lagoon (thermocline at 5 m) and three for the Bania Lake (thermoclines at 3 and 6 m), though these are just estimated thermoclines based on temperature shifts in the measured data, but the sampling resolution is too low to give exact thermocline depths.

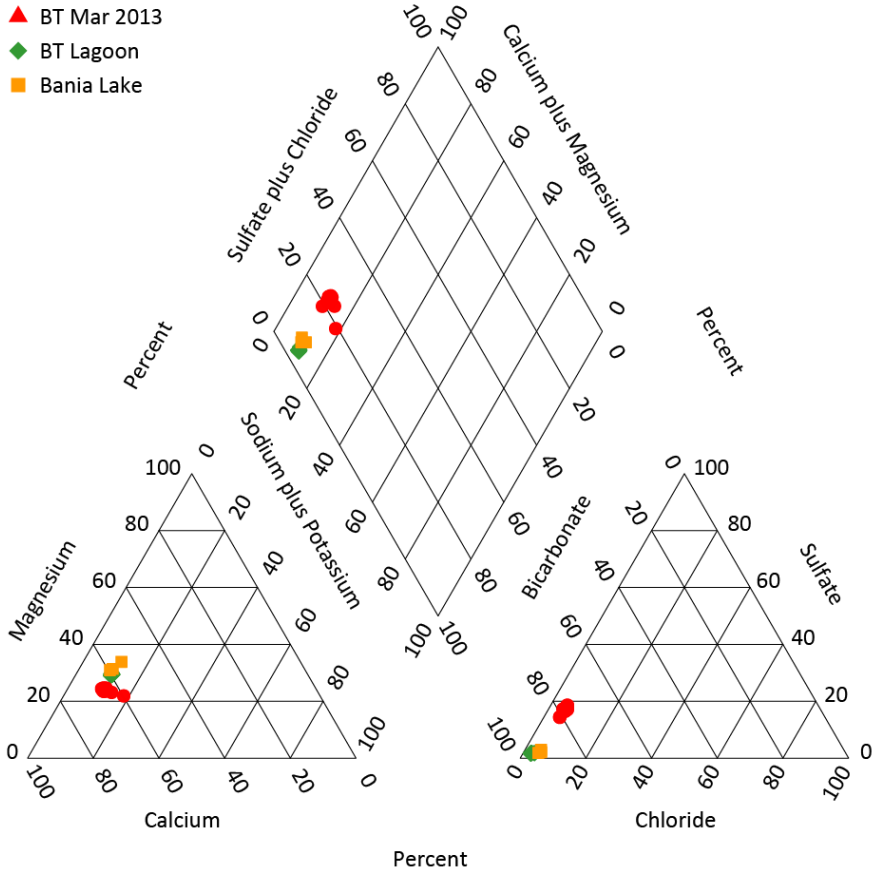


Figure 12: Piper (1944) Plot for all water samples of different sample sites. All samples are determined as Ca-Mg-HCO<sub>3</sub>-Type water

The hydrochemical compositions of all three sample sites (Lake Bol'shoe Toko, lagoon and Bania Lake) have similar values, visualized in a Piper plot (Figure 12) all samples plot roughly within  $60:35:15 \pm 5 \%$  ( $\text{Ca}^{2+}:\text{Mg}^{2+}:\text{K}^+ + \text{Na}^+$ ) of the cation composition triangle.

A similar pattern is shown for the anion composition. Here,  $\text{HCO}_3^-$  is dominant for all basins but there is a notable difference comparing the main basin of Lake Bol'shoe Toko with the lagoon and the side lake Bania Lake. Whereas the latter plot nearly at 100 %  $\text{HCO}_3^-$  (green diamonds and orange squares in Figure 12), samples taken from Lake Bol'shoe Toko (red triangles) have a minor content of sulfate and chloride ( $\text{HCO}_3^-/\text{SO}_4^{2-}/\text{Cl}^- = 80/17/3$  [%]).

The composite diamond plot clarifies that the basins only vary in their anion composition though all samples can be classified as Ca-Mg-  $\text{HCO}_3^-$ -type waters (according to Piper, 1944).

Regarding minor elements, in nearly all samples traces of aluminum (Al) and iron (Fe) have been found. Concentrations of manganese (Mn) were measured in water samples close to the bottom (in all basins). There was no evidence for significant concentrations of environmental relevant elements (Pb, Cr, V, Co, Ni, Cu).

For Lake Bol'shoe Toko, the highest concentrations of Aluminum (Al), Silicon (Si) and Strontium (Sr) concentrations were measured in surface samples with decreasing concentrations with depth, except for a concentration increase above the sediment surface. A similar picture is drawn for the lagoon, though here, in comparison with the main basin of Lake Bol'shoe Toko, less Al (50 % lower) but higher amounts of Si (1.5 times higher) and Sr (3 – 3.5 times higher) were measured.

For Bania Lake, it is hard to infer a general trend, regarding the low sample resolution, but the concentration of Al in waters is comparable to waters taken from the lagoon and its Sr concentration comparable to the once measured at Lake Bol'shoe Toko. Silicon concentrations are even lower than those measured at Lake Bol'shoe Toko.

The concentrations of sulfate ( $\text{SO}_4^{2-}$ ) follows the trend of Al (highest concentration at Bol'shoe Toko (2.4 mg/l), low concentration in the lagoon (0.5 mg/l) and Bania Lake (0.4 mg/l)) and the concentrations of nitrate ( $\text{NO}_3^-$ ) the mirror-inverted trend of Sr (higher concentrations in waters from Bol'shoe Toko and Bania Lake (both  $\approx 0.8$  mg/l) in comparison with water samples from the lagoon (0.3 mg/l)). There was no phosphorus found.

## 5 Discussion

In this chapter the results of the sample data from Lake Bol'shoe Toko are interpreted and discussed. Firstly, possible water and precipitation sources of the study area are examined, by comparing precipitation and snow data taken during the field campaign with data of Yakutsk from the Global Network of Isotopes in Precipitation (GNIP) and from Kloss (2008). Spatial variations in the isotopic and hydrochemical composition at Lake Bol'shoe Toko and its surroundings are discussed with regard to the geomorphological and geological setting. Furthermore, changes in the isotopic composition with depth are interpreted with respect to seasonal lake water stratification and fractionation processes. Lastly, the isotopic composition of Lake Bol'shoe Toko is discussed in the regional context, comparing it with two other lakes along a west-east transect of same latitude.

### 5.1 Water and precipitation sources for Lake Bol'shoe Toko

The isotopic signal measured in Central and East Siberian precipitation indicates a composite of moisture sources (Kurita et al., 2004). The precipitation is predominantly of western origin (Shahgedanova, 2002), hence moisture masses have been transported a far distance and are therefore depleted in heavy isotopes due to a combination of latitude effect and continental effect, the so called Rayleigh distillation (Rozanski et al., 1993, Kurita et al., 2004). However, secondary moisture sources have been reported to be the Arctic Ocean in the North and the Sea of Okhotsk in the East (Kurita, 2003, Kloss, 2008). Additionally, air mass movement towards the study site from the Sea of Okhotsk is likely, as the distance is only 300 km and the mountainous range does not exceed 1500 m. This could contribute to the higher annual mean precipitation at Lake Bol'shoe Toko (452 mm/year) compared to Yakutsk (250mm/year). Long-term mean surface winds indicate that during winter, such transport of air masses from the East is prevented by the Siberian anticyclone, whereas during summer months (June to July) westward transport of air and moisture from the Sea of Okhotsk land inwards occurs (Kurita, 2003, Lee et al., 2003). Although, this pattern of precipitation is still unclear (Kurita et al., 2004), it might be responsible for the high range in annual precipitation ( $\approx 232$  to  $\approx 640$  mm, Konstantinov (2000), NOAA record of Toko RS (1960-2015). Nonetheless, there is a pronounced seasonal signal within the isotopic composition of precipitation with isotopically light snow fall in winter and heavier isotopic composition in summer, that cannot be explained entirely by seasonal temperature variation (Kurita et al., 2004). This observation is supported

by models calculating the isotopic composition in precipitation (Bowen and Wilkinson, 2002, Bowen and Revenaugh, 2003, Bowen et al., 2005). The online isotopes in precipitation calculator (OIPC) predicts a mean annual  $\delta^{18}\text{O}$  signal of  $-14.9 \pm 0.8 \text{ ‰}$  and  $-113 \pm 6 \text{ ‰}$  in  $\delta\text{D}$ , respectively, for Lake Bol'shoe Toko (see Figure 13). However, models tend to underestimate isotopic depletion due to Rayleigh distillation of precipitation over Central and East Siberia (Butzin et al., 2014). When checking the model's consistency versus GNIP data taken at Yakutsk, this becomes evident. The OIPC calculates an annual mean of  $-14.5 \text{ ‰}$  in  $\delta^{18}\text{O}$  and  $-113 \text{ ‰}$  in  $\delta\text{D}$ , respectively, whereas annual means based on daily precipitation are  $-20 \text{ ‰}$  in  $\delta^{18}\text{O}$  and  $-158 \text{ ‰}$  in  $\delta\text{D}$ . Taking these shortcomings into consideration, models' calculated annual mean is comparable to the mean isotopic composition of Lake Bol'shoe Toko ( $-18.3 \pm 0.2 \text{ ‰}$  in  $\delta^{18}\text{O}$ ), supporting the hypothesis that Bol'shoe Toko's isotopic signal is directly link to precipitation.

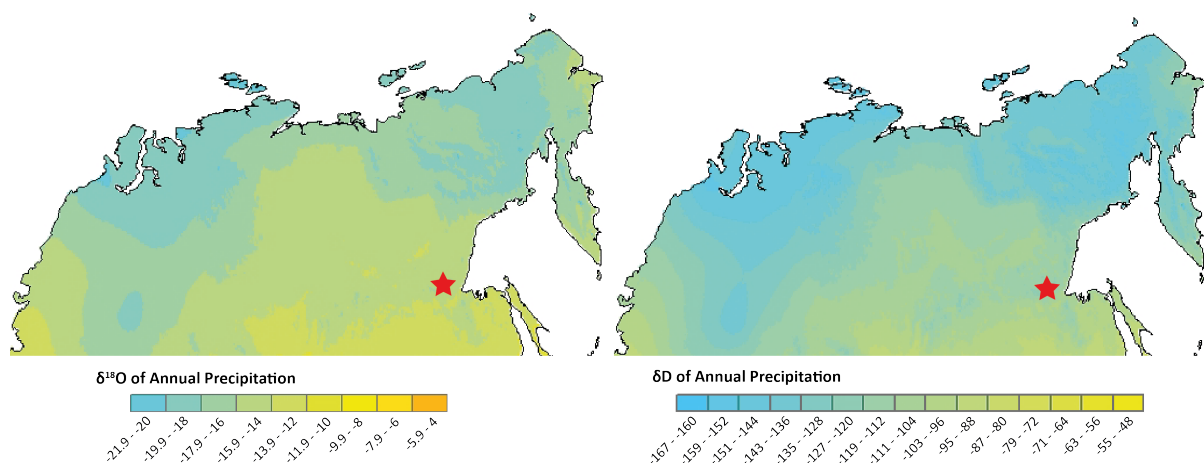


Figure 13: Annual mean  $\delta\text{D}$  and  $\delta^{18}\text{O}$  in precipitation patterns (Isoscapes) for North Asia. Red star shows study site (adopted after West et al., 2010).

Additionally, Bol'shoe Toko's main inflow, the Utuk River, springs in the Stanovoi mountains (peaks up to 2900 m) discharging meltwater and precipitation into the lake. As winter precipitation is isotopically lighter due to colder temperature during initial moisture formation (seasonality effect, e.g. Dansgaard, 1964, Rozanski et al., 1993), the resulting meltwaters are isotopically depleted. Furthermore, rainfall in the mountains is additionally depleted in heavy isotopes due to the altitude effect. Calculations from OIPC for the origin region of Utuk River<sup>1</sup>

<sup>1</sup> (coordinates: 55.888049° N, 130.453781° W, 1944 m altitude, sample point picked by tracing the Utuk river via satellite pictures (Google Earth)).

were  $-16.9 \pm 1.0 \text{ ‰}$  in  $\delta^{18}\text{O}$  and  $-128 \pm 8 \text{ ‰}$  in  $\delta\text{D}$ , respectively, indicating a depletion of  $\approx 2 \text{ ‰}$  in  $\delta^{18}\text{O}$ , compared to the predication for Lake Bol'shoe Toko ( $\delta^{18}\text{O} -14.9 \pm 0.8 \text{ ‰}$ ), due to higher altitudes (although the Rayleigh distillation is still underestimate). As a result of this isotopic depletion due to higher altitudes, river run-off into Lake Bol'shoe Toko leads to lighter isotopic composition of the lake water.

At Lake Bol'shoe Toko, several samples of snow covering the lake ice were sampled and one precipitation event (02 April 2013) was captured. The mean isotopic composition of these snow sample was  $-35.2 \pm 3.9 \text{ ‰}$  in  $\delta^{18}\text{O}$  and  $-266 \pm 30 \text{ ‰}$  in  $\delta\text{D}$ , respectively, which is comparable to winter precipitation measured at Yakutsk. Therefore, a similar moisture transportation path and conditions like origin over the North Atlantic with isotopic depletion over western Siberia and cold temperature can be assumed. The mean d-excess of snow of  $16 \pm 4 \text{ ‰}$  indicates arid and cold conditions at the moisture source. The high d-excess is in good agreement with snowpack analysis in eastern Siberia carried out by Kurita et al. (2005). Additionally, high d-excesses for the northern hemisphere and for both suggested moisture sources (North Atlantic and Sea of Okhotsk) were predicted by Pfahl and Sodemann (2014) during winter months (December to February).

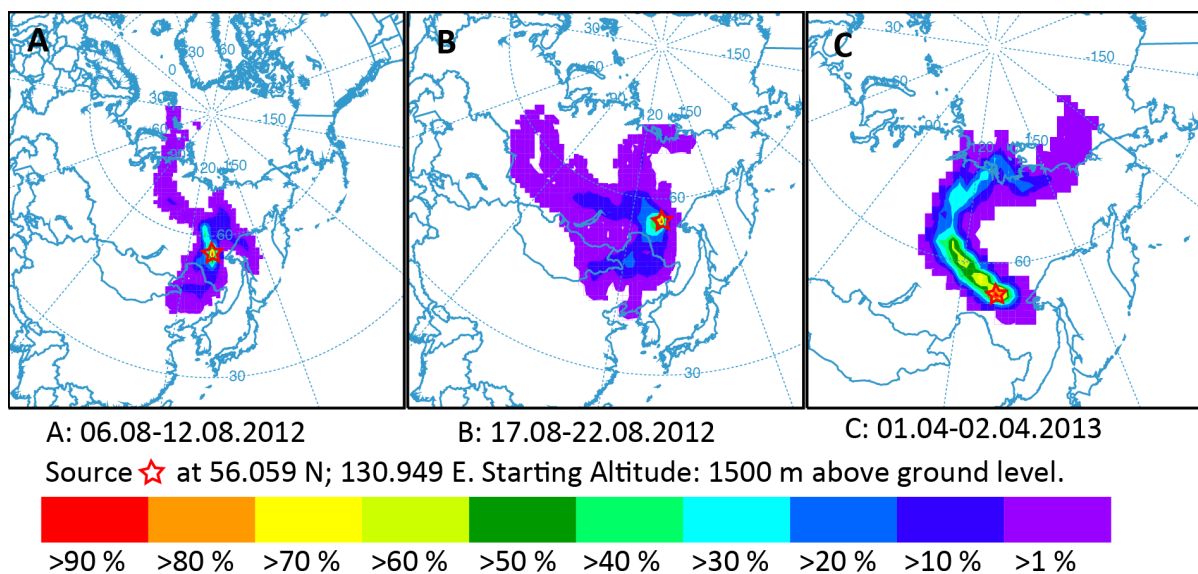


Figure 14: HYSPLIT back trajectory frequencies prior to both 6-day precipitation events in August 2012 (06-08.08.2012 (A), 17.-22.08.2012 (B)) and to the precipitation event 1-3 April 2013 (C). A new trajectory was started each 6 hand run for 120 h. Frequency calculate based on a 2 x 2 degree grid. Back trajectory frequencies indicate various moisture sources for the 06-08.08.2012 (A), whereas for 17.-22.08.2012 (B) and 1-3 April 2013 (C) a predominantly western origin is displayed.

Using NOAA HYSPLIT (Stein et al., 2015, Rolph, 2016), backwards trajectory frequencies for 120 h prior to the precipitation events on the 2 April 2013 during the March campaign as well as for two precipitation events in August 2012 were modelled. Whereas a predominantly western origin of the air mass for the precipitation event in April 2013 (see C in Figure 14) and for the event during 17 to 22 August 2012 (see B in Figure 14) is suggested, the model indicates various air mass origins during the 06 and 08 August 2012 (see A in Figure 14). This supports the assumption that moisture during summer may be brought from various source regions to Bol'shoe Toko. However, the branches of southern origin in A and B (Figure 14) can be excluded as moisture pathways, because Lake Bol'shoe Toko is shielded in the South by the Stanovoy mountain range.

In conclusion, due to lacking precipitation data over Siberia, a primary moisture source cannot be identified clearly. Both modelled summer and measured winter (snow) precipitation data indicate a composite of source moisture. However, literature reports primarily westerly influences, meaning that easterly and northerly sources might be of subordinate priority.

## 5.2 The isotopic signal of Lake Bol'shoe Toko and its spatial variations

Based on the surface waters, there is no evidence for significant spatial variations in the isotopic composition for Lake Bol'shoe Toko. However, two sample points near the shore in the South of Lake Bol'shoe Toko show slightly heavier isotopic compositions. This might be due to mixed-in isotopic signals of smaller creeks running into the lake.

The mean isotopic composition of the water profile at PG2208 ( $\delta^{18}\text{O}_{PG2208} = -18.2 \pm 0.2 \text{ ‰}$ ) is slightly heavier than the surface samples ( $\delta^{18}\text{O}_{surface} = -18.6 \pm 0.1 \text{ ‰}$ ) but this is explainable due to isotopic fractionation during ice formation. Heavier isotopes will preferably be turned into ice, resulting in a depletion of heavy isotopes in the surface water layer. For all samples, the mean value  $\delta^{18}\text{O}_{mean}$  is  $18.4 \pm 0.2 \text{ ‰}$ , although  $\delta^{18}\text{O}_{PG2208}$  might be more representable as fractionation influence is limited to the uppermost 10 m of the water column and Lake Bol'shoe Toko is deeper than 10 m for the majority of its extension.

The three sampled basins, however, have a distinct isotopic signal (Figure 7). The heaviest (highest) isotopic composition was measured at the much shallower and smaller side lake "Bania Lake" ( $\delta^{18}\text{O}_{Bania} = -16.1 \pm 0.2 \text{ ‰}$ ), whereas the lowest isotopic composition was measured at the lagoon ( $\delta^{18}\text{O}_{lagoon} = -18.9 \pm 0.2 \text{ ‰}$ ). Additionally, whereas waters taken from the lagoon and Lake Bol'shoe Toko are situated close to the GMWL, water from Bania Lake is

shifted underneath the GMWL and correlates better with the local meteoric water line (LMWL) of Yakutsk (see Figure 7). This is indicative that Bania Lake may be affected by evaporative enrichment during summer, while the lagoon and Bol'shoe Toko are not or at least not to a significant degree.

The low  $d\text{-excess}_{\text{Bania}}$  of  $-3 \text{ ‰}$  at Bania Lake supports this assumption, since lighter isotopes are preferentially evaporated. As a result, shallow basins get enriched in heavy isotopes due to evaporation which decreases the  $d\text{-excess}$  of the residue water. Consequently, during summer, the initial isotopically depleted melt-water feeding Bania Lake gets enriched as lighter waters are preferably turned into vapor. This enrichment is enhanced due to the shape of Bania Lake (shallow but relatively extensive basin). These evaporative enrichments are typical for closed-system lakes (e.g. Ichiyanagi et al., 2003, Mayr et al., 2007, Kostrova et al., 2013).

In contrast, the lagoon is isotopically slightly lighter ( $\delta^{18}\text{O}_{\text{lagoon}} = -18.9 \pm 0.2 \text{ ‰}$ ) than Bol'shoe Toko's main basin. Its mean isotopic composition shows a small difference of  $0.5 \text{ ‰}$  in  $\delta^{18}\text{O}$  and  $6 \text{ ‰}$  in  $\delta\text{D}$  compared to Lake Bol'shoe Toko. An unnamed river which discharges into the lagoon originates from a smaller lake ca. 5 km south east of Lake Bol'shoe Toko. Therefore, discharge into the lagoon is highest during melting season, bringing isotopically lighter waters into the lagoon. Due to its connection to Lake Bol'shoe Toko, the lagoon then acts like a through-flow system lake further outflowing water into Lake Bol'shoe Toko, which in turn levels their isotopic signal to some degree.

Although there was no evidence for evaporation effects found for Lake Bol'shoe Toko in the present system, this might have been different in the past. Löffler (2016) reported varying lake water levels over the last 19,500 years BP. Higher lake water level than present would result in the flooding of the relatively shallow bank in the eastern part of Lake Bol'shoe Toko, increasing the area of shallow water of the lake. Furthermore, it would result in a connection between Bania Lake and Lake Bol'shoe Toko. Such a connection was also hypothesized by Weniger (2016) during the Early Holocene and Mid-Holocene. For this epoch, Chironomids record, derived from a sediment core from Bania Lake, indicated 4-5 m higher water level compared to present Bania Lake, as well as colder water temperatures and oligotrophic conditions similar to present Lake Bol'shoe Toko. With the onset of the Late Holocene, lowering water levels led to the present separation of both lakes. Additionally, this area was reported as a lake terrace (Kornilov, 1962, Konstantinov, 2000) which supports this

hypothesis. An increase in shallow water area might have increase evaporation and thus leading to enrichment in heavy isotopes and hence higher  $\delta^{18}\text{O}$ -values, at least for surface waters in this specific areas. However, Löffler (2016) and Weniger (2016), both suggested higher inflow of cold melt water by the Utuk river due to glacial retreat during the Early and Mid-Holocene. Thus, the discharge of isotopically depleted water might have been higher than of the present system, opposing the effect of possible enhanced evaporative enrichment. In fact, if an increase in water discharge from the Stanovoi mountains was the main contributor to a water level rise of 4-5 m during Early and Mid-Holocene (as suggested by Weniger (2016)), the mean isotopic composition of Lake Bol'shoe Toko may have been lower than measured in the present lake.

### 5.3 Isotope-depth relationship at Lake Bolshoe Toko

The trend of all winter water depth profiles to lighter isotopic composition in the uppermost part is directly related to isotopic fractionation that accompanies ice cover formation. As ice is a state of aggregation with higher intermolecular bonding, heavier isotopes are preferentially turned into ice leaving the uppermost water layer (from which the ice is formed) isotopically depleted. Mixture of the depleted waters with the rest of the water column is

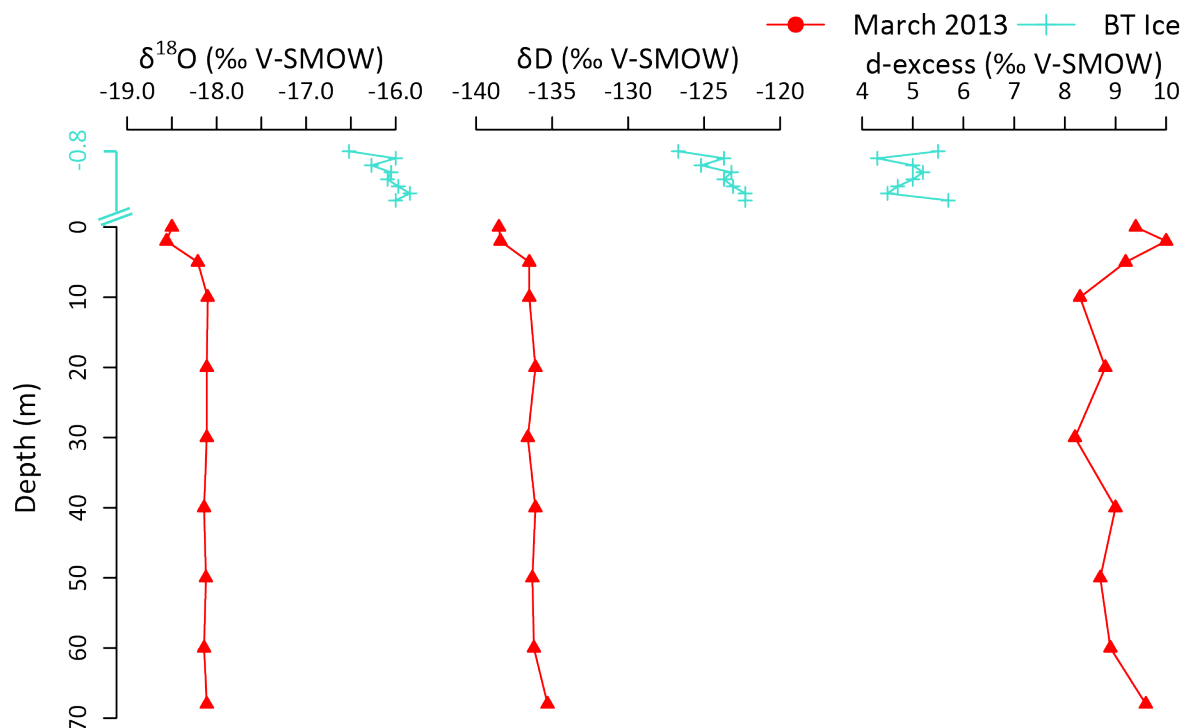


Figure 15: Isotope-depth profiles for both water (red) and lake ice (turquoise) at site PG2208, Lake Bol'shoe Toko taken in March 2013. Negative depth values display the thickness of the ice cover in m.

suppressed by temperature stratification under the ice which is distinct for Lake Bol'shoe Toko. A temperature increase from 2 m to 5 m was observed which correlates with the maximum shift in  $\delta^{18}\text{O}$  (0.35 ‰) and  $\delta\text{D}$  (1.9 ‰). For waters below the upper water layer (10 m for Lake Bol'shoe Toko) the isotope signal is uniform indicating a very well mixed water column with no isotopic stratification (Figure 15). This indicates that after thermal stratification the lake's water isotopic composition is not altered except during ice formation. For the August 2012 data, there is a more complex isotope-depth relationship. Although the waters mean isotopic composition of  $-18.2 \pm 0.3$  ‰ in  $\delta^{18}\text{O}$  and  $-137 \pm 2$  ‰ in  $\delta\text{D}$ , respectively, is the same as observed for waters taken in March 2013, the individual isotopic composition shows a zig-zag pattern (Figure 9). A similar mean isotopic composition indicates evaporation has not a strong effect and therefore there seems to be no strong seasonal change. This is typical for through-flow lakes (Mayr et al., 2007). However, the zig-zag pattern is unusual for this kind. Firstly, the uppermost 10 m are isotopically heavier than the water below. Although during evaporation lighter isotopes are preferentially turned into water vapor, leaving the remaining water enriched in heavy isotopes, this process can be excluded. Evaporation as a kinetic process is depended on e.g. relative humidity, wind shear and surface temperature and its signal is marked in characteristic evaporation lines when plotted in a  $\delta^{18}\text{O}$ -  $\delta\text{D}$  diagram. This means that the uppermost water samples would be situated along a line below the global meteoric water line (GMWL,  $\delta\text{D} = 8 * \delta^{18}\text{O} + 10$ ) with a slope  $< 8$ . In the August data, there were no such evaporation lines found. In contrast, the measured  $\delta^{18}\text{O}$  is close to the GMWL indicating an unaltered precipitation signal (see Figure 9). Additionally, evaporative enrichment during summer is pronounced for well thermal stratified lakes (dimictic) where mixing is prevented (Mayr et al., 2007). Such thermal stratification is weak at least in August 2012 indicating a cold polymictic lake.

Meteorological data from the nearby weather station (Toko RS, 10 km northward) recorded heavy rainfall for August 2012. Two 6 day-long precipitation events accounted for more rain than the August long-term mean. In total, August 2012 precipitation was 25 mm above the long term mean (83 mm). Such precipitation events could cause temporary isotopic stratification or a variation in the isotopic signal throughout the water column. Precipitation in summer has a heavier isotopic composition than the annual mean. Additionally, summer

rainfall is assumedly warmer than the water body of Lake Bol'shoe Toko, as it is fed by cold river run off from the mountains.

Thus, the thermal differences lead to different water layers, carrying slightly different isotopic signals. Due to ongoing mixing, these variations are then evened. In conclusion, such variations in the isotopic composition throughout the August profile are more a temporal phenomenon and not characteristic for Lake Bol'shoe Toko.

#### **5.4 Discussion of the hydrochemical composition**

The major ion composition (Figure 12) as well as the low conductivity of Lake Bol'shoe Toko, Bania Lake and the lagoon, point towards a lake system with water supply mainly from surface run-off and atmospheric precipitation and fresh water conditions. Furthermore, it indicates rock dominance of igneous rock type, especially for Lake Bol'shoe Toko (Wetzel, 2001).

The major cation composition of  $\text{Ca} \gg \text{Mg} > \text{Na} > \text{K}$ , however, contrasts this assumption, since magnesium concentrations are higher than sodium concentrations for all samples. Hence, a composite salinity source of igneous rocks overwritten by weathering of calcareous/sedimentary rocks is suggested. This is supported by the anion composition of  $\text{HCO}_3 \gg \text{SO}_4 > \text{Cl}$  at least for Lake Bol'shoe Toko, since sulfate influx is mainly due to weathering of rocks and soils.

In contrast, sulfate concentration at the lagoon and Bania Lake are lower than at Lake Bol'shoe Toko and the anion composition is shifted towards  $\text{HCO}_3 \gg \text{Cl} \geq \text{SO}_4$ , thus indicating a greater influence of a calcareous and salinity source. In fact, in the lagoon there is a notable overall increase of Ca, Mg and  $\text{HCO}_3$  concentrations resulting in higher salinity/conductivity. Conductivity and Ca, Mg and  $\text{HCO}_3$  concentrations of Bania Lake, however, show only a minor difference in comparison with Lake Bol'shoe Toko water.

Aforementioned differences in Ca, Mg,  $\text{SO}_4$  and bicarbonate can be either caused by changes of acidic precipitation (e.g. due to higher impact of the adjacent coal mining activity) in the corresponding water source regions or changes of the corresponding source elements in the bedrock or soil, respectively (mineral composition, e.g. calcite, pyrite in the rock). For the area of Lake Bol'shoe Toko, same acidic precipitation is assumed, since rivers running into both lagoon and Bol'shoe Toko are not of significant length. So, both drainage areas (for Lake Bol'shoe Toko and the lagoon, respectively) likely differ in their abundance of sulfuric minerals prone to weathering. This is an indication for changes of rock type for the drainage areas.

Consequently, based on the major ion composition, water supply from slightly different sources for each basin is suggested.

These differences are also reflected within the concentration of minor elements. Nitrate concentration of all three sample basins are within the global range for unpolluted freshwater (0.1-1 mg/l). However, concentrations of nitrate in the lagoon were  $\approx$ 50% lower (0.3 mg/l) than measured for Lake Bol'shoe Toko and the Bania Lake ( $\approx$ 0.8 mg/l). In conjunction with the non-presence of any phosphorus as additional nutrient, nitrate concentrations below 0.3 mg/l have significant impact on algae growth (Wetzel, 2001).

The higher Aluminium concentration in waters of Lake Bol'shoe Toko support the igneous rock influence of source water, whereas the distribution of silicon in water (primarily occurring as dissolved silicate), however, is contradictive at first glance. The enrichment in the lagoon due to stronger influx of silicon is unlikely, since sources of silicon are mainly silicate minerals. Nonetheless, the relative enrichment of silicon in the lagoon water may be due to inhibited uptake by e.g. diatoms, higher recycling rates of silicon from the sediments and/or prior enrichment in the pond feeding the lagoon. Lastly, higher strontium concentrations at the lagoon than measured at Lake Bol'shoe Toko or Bania Lake are corresponding with higher calcium and bicarbonate concentration, since strontium behaves geochemically similar to calcium and therefore is commonly associated with calcite (e.g. Odum, 1951, Faure, 1977).

In summary, the ionic composition of waters at Lake Bol'shoe Toko, lagoon and Bania Lake reflect the geomorphologic and geologic setting of the study area. The Utuk river which discharges into Lake Bol'shoe Toko springs in the predominantly mafic Stanovoi mountains and then runs over Cretaceous and Jurassic sedimentary rocks hence uptakes both signals due to weathering. In contrast, the unnamed river running into the lagoon carries no igneous signatures. But, since sedimentary deposits are more vulnerable to weathering than igneous rocks, the relative ion discharge of the unnamed river into the lagoon is higher than that Utuk river. Lastly, Bania Lake's ion composition supports the assumption of predominant input of atmospheric water and resulting nearby surface water discharge. As a result, water from Bania Lake shows slightly higher Ca, Mg,  $\text{HCO}_3$  concentrations than Bol'shoe Toko but lack the igneous signal of  $\text{SO}_4$ , Al and Si. Additionally, higher soil-water interaction before running into the corresponding lake basins is reflected in the iron and manganese signature of Bania Lake and lagoon water, as iron and manganese input is generally caused by anoxic weathering conditions of soils (Wetzel, 2001).

Generally, the uniformity of the ion composition along the water column and spatially in surface waters within their respective sample basins hints towards a well-mixed water body in winter time. The relative enrichment of ions in the surface layer compared to water taken from deeper water layers, which is reflected for all basins, is an effect of ice cover formation (leaving salts as residue in the surface water layer).

There was no evidence in the hydrochemical data for an impact on the lake ecosystem due to enhanced coal mining activity in the adjunct area, as presumed by Konstantinov (2000), as sulfate, nitrate and other related ions concentrations are below or within global average for unpolluted freshwaters.

Overall, the hydrochemistry data corresponds well with the isotope analysis and vice-versa. Based on both datasets, Lake Bol'shoe Toko and the lagoon can be characterized as a cold polymictic (stratified in winter, weak or non-stratified in summer), oligotrophic, open through-flow lake system. In contrast, Bania Lake is a closed system lake, effected by evaporation in summer and, based on lower oxygen concentrations (compared to Lake Bol'shoe Toko) and its shape, assumedly dimictic and eutrophic.

## **5.5 Lake Bol'shoe Toko in regional comparison**

To compare Lake Bol'shoe Toko with the regional setting of Siberian lakes, two previously investigated lakes of comparable climatic and geologic setting were chosen: Two-Yurts lake on Kamchatka Peninsula (Meyer et al., 2015) and Lake Kotokel (Kostrova et al., 2013), a side lake of Lake Baikal.

Although all three lakes are of similar latitude, they show significant differences in their isotopic compositions and its link to precipitation.

Bol'shoe Toko and Two-Yurts are isotopically non-stratified and well-mixed. Evaporative enrichment during summer is not present. Additionally, both lakes have low conductivities in common. Primarily responsible are their similar settings, as both are elongated through-flow lake system in a mountainous region. Two-Yurts Lake, as well as Lake Bol'shoe Toko, are predominantly fed by river run-off and precipitation resulting in a close link of the isotope signal between lake water and precipitation. Their waters are situated along the GMWL. However, Lake Bol'shoe Toko is isotopically lighter than Two-Yurts Lake, possibly due to its higher altitude (Bol'shoe Toko: 904 m a.s.l.; Two-Yurts Lake: 275 m a.s.l.) and different pathways of moisture. Two-Yurts lake has a more costal/maritime influenced climate (Meyer

et al., 2015), whereas at Lake Bol'shoe Toko continental climate is prevailing (Shahgedanova, 2002).

In contrast, Lake Kotokel represents partly a closed-system lake with notable evaporative enrichment. Its waters are shifted below the GMWL (Kostrova et al., 2013). However, Lake Bol'shoe Toko and Lake Kotokel share similar source water dynamics, since both lakes (as well as Two-Yurts lake) are mostly precipitation and meltwater influenced. The estimated original meteoric water prior to evaporation for Lake Kotokel is  $\approx -18.5$  ‰ in  $\delta^{18}\text{O}$  (Kostrova et al., 2013) which is comparable to Lake Bol'shoe Toko  $\delta^{18}\text{O}_{mean}$  of  $18.4 \pm 0.2$  ‰, indicating similar effects on the isotopic composition of moisture. This is not surprising, since both lakes get discharge from a mountainous region (Kostrova et al., 2013).

In summary, Lake Bol'shoe Toko shows similar characteristics of water source dynamics as Lake Kotokel (despite its evaporative enrichment) and Two-Yurts Lake. There is good correlation between lake water isotopes and isotopes in precipitation, especially for the two open through-flow lake systems.

## 6 Conclusions

The variability of isotopic and hydrochemical composition at Lake Bol'shoe Toko was assessed using stable water isotope and hydrochemical analysis. The results were then compared with the geomorphological and geological setting as well as regional data (GNIP, Two-Yurts Lake and Lake Kotokel).

Precipitation at Lake Bol'shoe Toko is assumedly of westerly origin with subordinate sources over the Arctic Ocean and Sea of Okhotsk. Due to its continental setting, the isotopic composition of precipitation is depleted in heavy isotopes and has a strong seasonal signal. However, this seasonality is not reflected in the isotopic composition of the lake, due to large amounts of riverine input of meltwater and a well-mixed water body. Furthermore, the isotopic compositions of Lake Bol'shoe Toko ( $\delta^{18}\text{O}_{\text{Bolshoe}} = -18.2 \pm 0.2 \text{ ‰}$ ) and the lagoon ( $\delta^{18}\text{O}_{\text{Bolshoe}} = -18.9 \pm 0.2 \text{ ‰}$ ) correspond with the GMWL and do not show evaporative enrichment. Both isotopic and hydrochemical data indicate atmospheric precipitation and meltwater as the main water source. Accordingly,  $\delta^{18}\text{O}_{\text{Bolshoe}}$  is directly linked to  $\delta^{18}\text{O}_{\text{precipitation}}$ . The water of Lake Bol'shoe Toko is well mixed and does not show significant isotopic stratification. Fractionation only affects the isotopic composition of the surface water during lake ice-cover formation where thermal stratification prevents mixing.

Overall, Lake Bol'shoe Toko, lagoon and Bania Lake show unpolluted freshwater conditions with low conductivity and corresponding ion concentrations below the global average. They are well saturated in  $\text{O}_2$ , neutral to slightly acidic and showed thermal stratification in winter. Although all waters can be characterized as Ca-Mg- $\text{HCO}_3$ -Type water, the three lake basins show distinct variations with regard to their major and minor ion composition. The lagoon has low nutrient concentrations, potentially inhibiting algae growth. These variations are directly linked to differences in water origin.

In summary, Lake Bol'shoe Toko is a cold polymictic, oligotrophic, open through-flow lake system. It is an undisturbed ecosystem, well suited for paleoclimate research.

## 7 Outlook

In further investigations on Bol'shoe Toko, the isotopic composition of biogenic silicate in diatoms in sediment surface samples will be analyzed (in process) and water/diatom isotopic fractionation to be determined. This combined data can then be used for paleoclimate reconstruction based on  $\delta^{18}\text{O}_{\text{diatoms}}$  in long sediment cores, since  $\delta^{18}\text{O}_{\text{diatoms}}$  is a proxy of lake water conditions (e.g. temperature) which are in turn linked to the local and regional climate patterns. Sediment cores of the lagoon and Bania Lake should be compared with sediments of Lake Bol'shoe Toko to get a better understanding of possible changes in lake water level and lake expanse. Future investigation should also account for changes in  $\delta^{18}\text{O}_{\text{water}}$  due to glacial advances and retreats, since large amounts of meltwater discharge may alter the isotopic composition of the lake water and hence influencing the link between isotopes in lake water and precipitation.

Furthermore, sedimentological data and bioindicators (e.g. diatoms) suggest that the northern part is influenced by runoff from the moraine. But more indicators (such as isotopes and hydrochemical data of recent water samples) are needed to get a better knowledge about the mechanisms. Additional water samples from inflow and outflow as well as a spatial set of summer surface water samples of lake Bol'shoe Toko would help acquiring better information about seasonal effects on water conditions and the isotopic composition.

## References

- ACIA, A. C. I. A. 2004. Impacts of a warming arctic: Arctic climate impact assessment. Cambridge University Press Cambridge, 144.
- ARAGUÁS-ARAGUÁS, L., FROELICH, K. & ROZANSKI, K. 1998. Stable isotope composition of precipitation over southeast Asia. *Journal of Geophysical Research*, 103, 28,721-28,742.
- BISKABORN, B. K., HERZSCHUH, U., BOLSHIYANOV, D., SAVELIEVA, L. & DIEKMANN, B. 2012. Environmental variability in northeastern Siberia during the last ≈13,300 yr inferred from lake diatoms and sediment–geochemical parameters. *Palaeogeography, Palaeoclimatology, Palaeoecology*, 329, 22-36.
- BISKABORN, B. K., HERZSCHUH, U., BOLSHIYANOV, D., SAVELIEVA, L., ZIBULSKI, R. & DIEKMANN, B. 2013. Late Holocene thermokarst variability inferred from diatoms in a lake sediment record from the Lena Delta, Siberian Arctic. *Journal of paleolimnology*, 49, 155-170.
- BISKABORN, B. K., SUBETTO, D., SAVELIEVA, L., VAKHRAMEEVA, P. S., HANSCH, A., HERZSCHUH, U., KLEMM, J., HEINECKE, L., PESTRYAKOVA, L. & MEYER, H. 2016. Late Quaternary vegetation and lake system dynamics in north-eastern Siberia: Implications for seasonal climate variability. *Quaternary Science Reviews*, 147, 406-421.
- BOWEN, G. J. & REVENAUGH, J. 2003. Interpolating the isotopic composition of modern meteoric precipitation. *Water Resources Research*, 39, 1299.
- BOWEN, G. J., WASSENAAR, L. I. & HOBSON, K. A. 2005. Global application of stable hydrogen and oxygen isotopes to wildlife forensics. *Oecologia*, 143, 337-348.
- BOWEN, G. J. & WILKINSON, B. 2002. Spatial distribution of  $\delta^{18}\text{O}$  in meteoric precipitation. *Geology*, 30, 315-318.
- BUTZIN, M., WERNER, M., MASSON-DELMOTTE, V., RISI, C., FRANKENBERG, C., GRIBANOV, K., JOUZEL, J. & ZAKHAROV, V. I. 2014. Variations of oxygen-18 in West Siberian precipitation during the last 50 years. *Atmospheric Chemistry and Physics*, 14, 5853-5869.
- CLARK, I. D. & FRITZ, P. 1997. *Environmental isotopes in hydrogeology*, CRC press.
- CRAIG, H. 1961a. Isotopic variations in meteoric waters. *Science*, 133, 1702-1703.
- CRAIG, H. 1961b. Standard for reporting concentrations of deuterium and oxygen-18 in natural waters. *Science*, 133, 1833-1834.

- CRAIG, H. & GORDON, L. I. 1965. Deuterium and oxygen 18 variations in the ocean and the marine atmosphere. *In: TONGIORGI, E. (ed.) Stable isotopes in oceanographic studies and paleotemperatures. Proceedings of the Spoleto Conferences in Nuclear Geology.* Lischi e F., Pisa, pp. 9-130.
- DANSGAARD, W. 1964. Stable isotopes in precipitation. *Tellus*, 16, 436-468.
- DINCER, T. 1968. The use of oxygen 18 and deuterium concentrations in the water balance of lakes. *Water Resources Research*, 4, 1289-1306.
- DRESSLE, A. 2016. *The influence of recent climate change on spatial temporal diatom variability in Lake Bolshoe Toko, South Eastern Yakutia, Russia.* Master thesis.
- FAURE, G. 1977. Principles of isotope geology. New York, NY: John Wiley and Sons, Inc.
- GAT, J. R. 1995. Stable Isotopes of Fresh and Saline Lakes. *In: LERMAN, A., IMBODEN, D. M. & GAT, J. R. (eds.) Physics and Chemistry of Lakes.* Berlin, Heidelberg: Springer Berlin Heidelberg, pp. 139-165.
- GAVRILOVA, M. 1993. Climate and permafrost. *Permafrost and Periglacial Processes*, 4, 99-111.
- GIBSON, J., PREPAS, E. & MCEACHERN, P. 2002. Quantitative comparison of lake throughflow, residency, and catchment runoff using stable isotopes: modelling and results from a regional survey of Boreal lakes. *Journal of Hydrology*, 262, 128-144.
- GIBSON, J. J. & REID, R. 2010. Stable isotope fingerprint of open-water evaporation losses and effective drainage area fluctuations in a subarctic shield watershed. *Journal of Hydrology*, 381, 142-150.
- GIORGETTA, M. A., JUNGCLAUS, J., REICK, C. H., LEGUTKE, S., BADER, J., BÖTTINGER, M., BROVKIN, V., CRUEGER, T., ESCH, M., FIEG, K., GLUSHAK, K., GAYLER, V., HAAK, H., HOLLWEG, H.-D., ILYINA, T., KINNE, S., KORNBUEH, L., MATEI, D., MAURITSEN, T., MIKOLAJEWICZ, U., MUELLER, W., NOTZ, D., PITHAN, F., RADDATZ, T., RAST, S., REDLER, R., ROECKNER, E., SCHMIDT, H., SCHNUR, R., SEGSCHNEIDER, J., SIX, K. D., STOCKHAUSE, M., TIMMRECK, C., WEGNER, J., WIDMANN, H., WIENERS, K.-H., CLAUSSEN, M., MAROTZKE, J. & STEVENS, B. 2013. Climate and carbon cycle changes from 1850 to 2100 in MPI-ESM simulations for the Coupled Model Intercomparison Project phase 5. *Journal of Advances in Modeling Earth Systems*, 5, 572-597.
- HOEFS, J. 2015. Isotope fractionation processes of selected elements. *Stable Isotope Geochemistry.* Springer.
- ICHIYANAGI, K., SUGIMOTO, A., NUMAGUTI, A., KURITA, N., ISHII, Y. & OHATAI, T. 2003. Seasonal variation in stable isotopic composition of alaskian lake water near Yakutsk, Eastern Siberia. *Geochemical journal*, 37, 519-530.

- IMAEVA, L. P., IMAEV, V. S., KOZ'MIN, B. M. & MACKEY, K. 2009. Formation dynamics of fault-block structures in the eastern segment of the Baikal-Stanovoi seismic belt. *Izvestiya, Physics of the Solid Earth*, 45, 1006-1011.
- JENSEN, R. G., SHABAD, T. & WRIGHT, A. W. 1983. *Soviet natural resources in the world economy*, University of Chicago Press.
- KLOSS, A. L. 2008. *Water isotope geochemistry of recent precipitation in Central and North Siberia as a proxy for the local and regional climate system*. Diplomarbeit, Leibniz Universität Hannover.
- KONSTANTINOV, A. F. 2000. Environmental problems of lake Bolshoe Toko (in Russian). In: ZHIRKOV, I. I., PESTRYAKOVA, L.A., MAKSIMOV, G.N. (ed.) *Lakes of Cold Environments, part V: Resource Study, Resource Use, Ecology and Nature Protection Issue*. Yakutsk, Russia: Yakutsk State University Publishing House.
- KORNILOV, B. 1962. *Relief: The southeast suburbs of Aldan Mountains (in russian)*. Moscow, Publishing House of Academy of Sciences of the USSR.
- KOSTROVA, S. S., MEYER, H., CHAPLIGIN, B., KOSSLER, A., BEZRUKOVA, E. V. & TARASOV, P. E. 2013. Holocene oxygen isotope record of diatoms from Lake Kotokel (southern Siberia, Russia) and its palaeoclimatic implications. *Quaternary International*, 290-291, 21-34.
- KURITA, N. 2003. Relationship between the variation of isotopic ratios and the source of summer precipitation in eastern Siberia. *Journal of Geophysical Research*, 108.
- KURITA, N., SUGIMOTO, A., FUJII, Y., FUKAZAWA, T., MAKAROV, V. N., WATANABE, O., ICHIYANAGI, K., NUMAGUTI, A. & YOSHIDA, N. 2005. Isotopic composition and origin of snow over Siberia. *Journal of Geophysical Research: Atmospheres*, 110.
- KURITA, N., YOSHIDA, N., INOUE, G. & CHAYANOVA, E. A. 2004. Modern isotope climatology of Russia, A first assessment. *Journal of Geophysical Research*, 109, D03102, doi:10.1029/2003JD003404.
- LEE, K.-S., GRUNDSTEIN, A. J., WENNER, D. B., CHOI, M.-S., WOO, N.-C. & LEE, D.-H. 2003. Climatic controls on the stable isotopic composition of precipitation in Northeast Asia. *Climate Research*, 23, 137-148.
- LENG, M. J. & BARKER, P. A. 2006. A review of the oxygen isotope composition of lacustrine diatom silica for palaeoclimate reconstruction. *Earth-Science Reviews*, 75, 5-27.
- LÖFFLER, T. 2016. *Late Quaternary Depositional Environment of Lake Bolshoe Toko, Yakutia, Russia*. Master thesis, University of Potsdam.

- MAYR, C., LÜCKE, A., STICHLER, W., TRIMBORN, P., ERCOLANO, B., OLIVA, G., OHLENDORF, C., SOTO, J., FEY, M., HABERZETTL, T., JANSSEN, S., SCHÄBITZ, F., SCHLESER, G. H., WILLE, M. & ZOLITSCHKA, B. 2007. Precipitation origin and evaporation of lakes in semi-arid Patagonia (Argentina) inferred from stable isotopes ( $\delta^{18}\text{O}$ ,  $\delta^2\text{H}$ ). *Journal of Hydrology*, 334, 53-63.
- MERLIVAT, L. & JOUZEL, J. 1979. Global climatic interpretation of the deuterium-oxygen 18 relationship for precipitation. *Journal of Geophysical Research: Oceans*, 84, 5029-5033.
- MEYER, H., CHAPLIGIN, B., HOFF, U., NAZAROVA, L. & DIEKMANN, B. 2015. Oxygen isotope composition of diatoms as Late Holocene climate proxy at Two-Yurts Lake, Central Kamchatka, Russia. *Global and Planetary Change*, 134, 118-128.
- MEYER, H., SCHÖNICKE, L., WAND, U., HUBBERTEN, H.-W. & FRIEDRICHSEN, H. 2000. Isotope studies of hydrogen and oxygen in ground ice-experiences with the equilibration technique. *Isotopes in Environmental and Health Studies*, 36, 133-149.
- MILLER, G. H., BRIGHAM-GRETTE, J., ALLEY, R., ANDERSON, L., BAUCH, H. A., DOUGLAS, M., EDWARDS, M., ELIAS, S., FINNEY, B. & FITZPATRICK, J. 2010. Temperature and precipitation history of the Arctic. *Quaternary Science Reviews*, 29, 1679-1715.
- NAZAROVA, L., LÜPFERT, H., SUBETTO, D., PESTRYAKOVA, L. & DIEKMANN, B. 2013. Holocene climate conditions in central Yakutia (Eastern Siberia) inferred from sediment composition and fossil chironomids of Lake Temje. *Quaternary International*, 290, 264-274.
- NÖLTE, J. 2002. ICP Emissionsspektrometrie für Praktiker. *Grundlagen, Methodenentwicklung, Anwendungsbeispiele*, Verlag Wiley-VCH, Weinheim, 3-527.
- ODUM, H. T. 1951. The stability of the world strontium cycle. *Science*, 114, 407-411.
- PARNACHEV, V. P. & DEGERMENDZHAY, A. G. 2002. Geographical, geological and hydrochemical distribution of saline lakes in Khakasia, Southern Siberia. *Aquatic ecology*, 36, 107-122.
- PFAHL, S. & SODEMANN, H. 2014. What controls deuterium excess in global precipitation? *Climate of the Past*, 10, 771-781.
- PIPER, A. M. 1944. A graphic procedure in the geochemical interpretation of water-analyses. *Eos, Transactions American Geophysical Union*, 25, 914-928.
- REIMANN, C., BANKS, D., BOGATYREV, I., CARITAT, P. D., KASHULINA, G. & NISKAVAARA, H. 1999. Lake water geochemistry on the western Kola Peninsula, north-west Russia. *Applied Geochemistry*, 14, 787-805.

- ROGORA, M., MOSELLO, R. & ARISCI, S. 2003. The effect of climate warming on the hydrochemistry of alpine lakes. *Water, Air, and Soil Pollution*, 148, 347-361.
- ROLPH, G. 2016. Real-time Environmental Applications and Display sYstem (READY) Website (<http://ready.arl.noaa.gov>). NOAA Air Resources Laboratory, Silver Spring. *Silver Spring, MD*.
- ROZANSKI, K., ARAGUÁS-ARAGUÁS, L. & GONFIANTINI, R. 1993. Isotopic patterns in modern global precipitation. 1-36.
- SCHLEUSNER, P., BISKABORN, B. K., KIENAST, F., WOLTER, J., SUBETTO, D. & DIEKMANN, B. 2015. Basin evolution and palaeoenvironmental variability of the thermokarst lake El'gene-Kyuele, Arctic Siberia. *Boreas*, 44, 216-229.
- SCHUUR, E. A. & ABBOTT, B. 2011. Climate change: High risk of permafrost thaw. *Nature*, 480, 32-33.
- SHAHGEDANOVA, M. 2002. Climate at present and in the historical past. In: SHAHGEDANOVA, M. (ed.) *The physical geography of northern Eurasia*. New York, NY, USA: Oxford University Press.
- STEIN, A., DRAXLER, R., ROLPH, G., STUNDER, B., COHEN, M. & NGAN, F. 2015. NOAA's HYSPLIT atmospheric transport and dispersion modeling system. *Bulletin of the American Meteorological Society*, 96, 2059-2077.
- WALTER, H. & LIETH, H. 1960. Klimadiagramm-Weltatlas. *Gustav Fischer Verlag, Jena*.
- WENIGER, L. 2016. *Holocene climate and environmental changes inferred from a subfossil chironomid record in a small lake near Bolshoe Toko, southeastern Yakutia (Russia)*. Master Thesis.
- WEST, J. B., BOWEN, G. J., DAWSON, T. E. & TU, K. P. 2010. *Understanding movement, pattern, and process on Earth through isotope mapping*, New York: Springer.
- WETZEL, R. G. 2001. *Limnology: lake and river ecosystems*, Gulf Professional Publishing.
- WOLLENWEBER, W. 2017, in prep. *Stable isotope analyses of biogenic opal from lacustrine sediments of Bolshoe Toko in southern Yakutia*. Master Master thesis.
- ZHANG, T., HEGINBOTTOM, J., BARRY, R. G. & BROWN, J. 2000. Further statistics on the distribution of permafrost and ground ice in the Northern Hemisphere 1. *Polar geography*, 24, 126-131.
- ZUBER, A. 1983. On the environmental isotope method for determining the water balance components of some lakes. *Journal of Hydrology*, 61, 409-427.

## Appendix

Table 3: Isotopic composition of snow and ice samples taken at Lake Bol'shoe Toko.

| Site   | $\delta^{18}\text{O}$ [‰] vs.<br>VSMOW | $\delta\text{D}$ [‰] vs.<br>VSMOW | d-excess [‰] vs.<br>VSMOW |
|--|--|-----------------------------------|---------------------------|
| Snow cover samples from various locations                  |  |                                   |                           |
| PG2206, 0-33 cm  | -33.45                                 | -257.0                            | 10.5                      |
| PG2116-X13   | -35.86                                 | -268.7                            | 18.2                      |
| PG2116-X16   | -37.95                                 | -285.2                            | 18.4                      |
| PG2122, 0-21 cm  | -36.86                                 | -283.5                            | 11.5                      |
| PG2122, 21-31 cm   | -41.14                                 | -306.9                            | 22.2                      |
| PG2122, 31-47 cm   | -30.43                                 | -227.9                            | 15.5                      |
| Precipitation, collected during snow fall on 02 April 2013 |  |                                   |                           |
| BT Snow 02.04.2013   | -30.81                                 | -229.4                            | 17.0                      |
| Surface ice samples  |  |                                   |                           |
| PG2116-X13   | -15.38                                 | -115.3                            | 7.8                       |
| PG2116-X16   | -14.95                                 | -111.1                            | 8.5                       |
| PG2208, ice core, numbers indicate depth in cm             |  |                                   |                           |
| 0-10   | -16.52                                 | -126.7                            | 5.5                       |
| 10-20  | -16.00                                 | -123.7                            | 4.3                       |
| 20-30  | -16.27                                 | -125.2                            | 5.0                       |
| 30-40  | -16.05                                 | -123.2                            | 5.2                       |
| 40-50  | -16.09                                 | -123.7                            | 5.0                       |
| 50-60  | -15.97                                 | -123.1                            | 4.7                       |
| 60-70  | -15.84                                 | -122.3                            | 4.5                       |
| 70-82  | -16.00                                 | -122.3                            | 5.7                       |

Table 4: Isotope and hydrochemistry data for all water samples taken in March 2013 (continues on page XI).

| Sample depth<br>[m]                                  | $\delta^{18}\text{O}$ [‰] vs.<br>VSMOW | $\delta\text{D}$ [‰] vs.<br>VSMOW | d-excess [‰] vs.<br>VSMOW | Temperature<br>[°C] | Oxygen content<br>[%] | Conductivity<br>[ $\mu\text{S}/\text{cm}$ ] | pH  | $\text{Ca}^{2+}$<br>[mg/l] | $\text{Mg}^{2+}$<br>[mg/l] | $\text{Na}^+$<br>[mg/l] |
|--|--|-----------------------------------|---------------------------|---------------------|-----------------------|---|-----|----------------------------|----------------------------|-------------------------|
| PG2208, water depth profile of Lake Bol'shoe Toko    |  |                                   |                           |                     |                       |   |     |                            |                            |                         |
| 0  | -18.5                                  | -138.5                            | 9.4                       | 0.5                 | 110.9                 | 35.1  | 6.8 | 4.73                       | 1.09                       | 0.78                    |
| 2  | -18.56                                 | -138.4                            | 10                        | 0.5                 | 119.9                 | 35.6  | 7.0 | 4.69                       | 1.07                       | 0.72                    |
| 5  | -18.21                                 | -136.5                            | 9.2                       | 1.5                 | 110.4                 | 32.1  | 7.1 | 4.10                       | 0.90                       | 0.64                    |
| 10   | -18.1                                  | -136.5                            | 8.3                       | 1.8                 | 108.9                 | 29.5  | 7.0 | 3.82                       | 0.86                       | 0.55                    |
| 20   | -18.11                                 | -136.1                            | 8.8                       | 2.5                 | 111.6                 | 31.2  | 7.0 | 3.84                       | 0.84                       | 0.61                    |
| 30   | -18.11                                 | -136.6                            | 8.2                       | 2.5                 | 108.1                 | 29.7  | 7.0 | 3.89                       | 0.87                       | 0.57                    |
| 40   | -18.14                                 | -136.1                            | 9                         | 2.5                 | 111.5                 | 29.1  | 6.9 | 3.81                       | 0.84                       | 0.63                    |
| 50   | -18.12                                 | -136.3                            | 8.7                       | 4                   | 102.4                 | 29.9  | 7.0 | 3.71                       | 0.84                       | 0.63                    |
| 60   | -18.14                                 | -136.2                            | 8.9                       | 4                   | 101.9                 | 30.8  | 7.0 | 3.84                       | 0.87                       | 0.54                    |
| 68   | -18.11                                 | -135.3                            | 9.6                       | 4                   | 101.3                 | 32.1  | 6.7 | 4.10                       | 0.91                       | 1.13                    |
| PG2122, water depth profile of the lagoon            |  |                                   |                           |                     |                       |   |     |                            |                            |                         |
| 0  | -19.21                                 | -145.3                            | 8.4                       | 0.5                 | 108.4                 | 67.8  | 7.0 | 9.01                       | 2.71                       | 1.61                    |
| 2  | -19.00                                 | -144.0                            | 8.0                       | 0.5                 | 115.0                 | 66.0  | 7.0 | 8.52                       | 2.56                       | 1.59                    |
| 5  | -18.88                                 | -143.6                            | 7.4                       | 2.5                 | 103.7                 | 61.0  | 7.0 | 7.99                       | 2.39                       | 1.48                    |
| 10   | -18.80                                 | -143.7                            | 6.7                       | 2.8                 | 106.7                 | 60.3  | 6.9 | 7.73                       | 2.36                       | 1.40                    |
| 18   | -18.85                                 | -143.9                            | 6.9                       | 3.0                 | 88.6                  | 67.4  | 6.7 | 8.48                       | 2.48                       | 1.54                    |
| PG2131, water depth profile of Bania Lake            |  |                                   |                           |                     |                       |   |     |                            |                            |                         |
| 0  | -16.22                                 | -131.8                            | -2.0                      | 0.5                 | 92.5                  | 42.6  | 6.5 | 5.44                       | 2.05                       | 1.10                    |
| 3  | -15.92                                 | -130.0                            | -2.6                      | 2.5                 | 92.1                  | 38.7  | 6.4 | 4.69                       | 1.48                       | 0.71                    |
| 6  | -16.01                                 | -130.9                            | -2.9                      | 4.0                 | 92.9                  | 40.0  | 6.5 | 4.82                       | 1.57                       | 0.78                    |
| Surface Samples, PG-number indicates sample location |  |                                   |                           |                     |                       |   |     |                            |                            |                         |
| PG2116-X13   | -18.48                                 | -138.5                            | 9.3                       | na                  | 99.4                  | 42.9  | 6.9 | 5.52                       | 1.23                       | 1.07                    |
| PG2116-X14   | -18.59                                 | -138.6                            | 10.1                      | na                  | 96.2                  | 42.5  | 6.8 | 5.26                       | 1.20                       | 0.83                    |
| PG2124   | -18.63                                 | -139.4                            | 9.7                       | na                  | 110.4                 | 37.9  | 7.0 | 4.68                       | 1.07                       | 0.77                    |
| PG2125   | -18.43                                 | -138.2                            | 9.2                       | na                  | 108.9                 | 39.1  | 7.2 | 4.91                       | 1.13                       | 0.79                    |
| PG2126   | -18.71                                 | -139.3                            | 10.4                      | na                  | 113.1                 | 36.6  | 7.1 | 4.70                       | 1.10                       | 0.76                    |
| PG2204   | -18.68                                 | -140.0                            | 9.5                       | na                  | 104.8                 | 38.5  | 6.9 | 5.03                       | 1.16                       | 0.79                    |
| PG2207   | -18.72                                 | -140.2                            | 9.6                       | na                  | 100.9                 | 38.4  | 6.9 | 5.00                       | 1.16                       | 0.74                    |

Table 5: Hydrochemistry data for all water samples taken in March 2013 continuation of Table 4.

| Sample depth<br>[m]                                  | K <sup>+</sup><br>[mg/l] | HCO <sub>3</sub> <sup>-</sup><br>[mg/l] | SO <sub>4</sub> <sup>2-</sup><br>[mg/l] | Cl <sup>-</sup><br>[mg/l] | Si<br>[mg/l] | NO <sub>3</sub> <sup>-</sup><br>[mg/l] | Al<br>[µg/l] | Sr<br>[µg/l] | Fe<br>[µg/l] | Mn<br>[µg/l] |
|--|--------------------------|---|---|---------------------------|--------------|--|--------------|--------------|--------------|--------------|
| PG2208, water depth profile for Lake Bol'shoe Toko   |                          |   |   |                           |              |  |              |              |              |              |
| 0  | 0.36                     | 13.58                                   | 2.47                                    | 0.51                      | 1.93         | 0.82                                   | 79.88        | 25.86        | 26.90        | < 20         |
| 2  | 0.34                     | 13.12                                   | 2.51                                    | 0.50                      | 1.91         | 0.82                                   | 77.06        | 24.85        | 29.06        | < 20         |
| 5  | 0.29                     | 12.81                                   | 2.17                                    | 0.49                      | 1.74         | 0.67                                   | 69.52        | 22.44        | 24.34        | < 20         |
| 10   | 0.27                     | 11.90                                   | 2.10                                    | 0.49                      | 1.63         | 0.62                                   | 62.67        | 20.69        | < 20         | < 20         |
| 20   | 0.28                     | 12.36                                   | 2.05                                    | 0.49                      | 1.64         | 0.66                                   | 64.51        | 20.74        | 20.89        | < 20         |
| 30   | 0.28                     | 11.44                                   | 1.99                                    | 0.50                      | 1.60         | 0.72                                   | 64.63        | 20.54        | 25.16        | < 20         |
| 40   | 0.28                     | 12.36                                   | 2.06                                    | 0.50                      | 1.64         | 0.64                                   | 66.36        | 20.87        | 26.56        | < 20         |
| 50   | 0.28                     | 11.44                                   | 2.03                                    | 0.49                      | 1.62         | 0.67                                   | 61.63        | 20.26        | < 20         | < 20         |
| 60   | 0.27                     | 14.03                                   | 1.96                                    | 0.49                      | 1.69         | 0.70                                   | 59.92        | 21.18        | 24.01        | < 20         |
| 68   | 0.53                     | 14.19                                   | 2.01                                    | 0.49                      | 1.85         | 0.69                                   | 75.55        | 22.68        | 282.36       | 416.97       |
| PG2122, water depth profile of the lagoon            |                          |   |   |                           |              |  |              |              |              |              |
| 0  | 0.40                     | 37.52                                   | 0.51                                    | 0.55                      | 3.01         | 0.29                                   | 43.19        | 90.57        | 147.56       | < 20         |
| 2  | 0.40                     | 35.85                                   | 0.48                                    | 0.53                      | 2.92         | 0.25                                   | 39.73        | 86.24        | 142.65       | < 20         |
| 5  | 0.38                     | 33.10                                   | 0.52                                    | 0.51                      | 2.71         | 0.28                                   | 41.63        | 80.10        | 132.91       | < 20         |
| 10   | 0.34                     | 32.64                                   | 0.48                                    | 0.69                      | 2.63         | 0.33                                   | 36.30        | 78.01        | 131.20       | < 20         |
| 18   | 0.36                     | 36.46                                   | 0.53                                    | 0.52                      | 3.10         | 0.40                                   | 29.50        | 86.03        | 361.36       | 375.28       |
| PG2131, water depth profile of Bania Lake            |                          |   |   |                           |              |  |              |              |              |              |
| 0  | 0.40                     | 21.81                                   | 0.55                                    | 0.67                      | 1.27         | 0.70                                   | 42.05        | 35.17        | 180.94       | < 20         |
| 3  | 0.27                     | 17.69                                   | 0.32                                    | 0.59                      | 1.21         | 0.89                                   | 37.45        | 27.86        | 308.01       | 77.26        |
| 6  | 0.32                     | 18.61                                   | 0.29                                    | 0.53                      | 1.41         | 0.94                                   | 35.95        | 29.64        | 451.89       | 84.19        |
| Surface Samples, PG-number indicates sample location |                          |   |   |                           |              |  |              |              |              |              |
| PG2116-X13   | 0.58                     | 16.78                                   | 2.96                                    | 0.71                      | 2.30         | 0.83                                   | 73.16        | 28.59        | 132.97       | 20.05        |
| PG2116-X14   | 0.41                     | 16.47                                   | 2.91                                    | 0.67                      | 2.27         | 0.85                                   | 71.75        | 27.57        | 124.64       | < 20         |
| PG2124   | 0.36                     | 14.80                                   | 2.66                                    | 0.60                      | 1.98         | 0.82                                   | 75.54        | 26.28        | 24.96        | < 20         |
| PG2125   | 0.40                     | 15.41                                   | 2.95                                    | 0.60                      | 2.05         | 0.88                                   | 73.31        | 26.29        | 33.13        | < 20         |
| PG2126   | 0.37                     | 15.10                                   | 2.77                                    | 0.58                      | 2.05         | 0.89                                   | 77.62        | 26.07        | 22.22        | < 20         |
| PG2204   | 0.39                     | 15.56                                   | 2.71                                    | 0.54                      | 2.13         | 0.74                                   | 84.78        | 27.42        | 24.22        | < 20         |
| PG2207   | 0.37                     | 15.71                                   | 2.72                                    | 0.51                      | 2.11         | 0.82                                   | 82.18        | 27.40        | 24.56        | < 20         |

Table 6: Isotope data for water samples taken in August 2012 (sampled by Pestryakova, measured at AWI Laboratory)

| Sample depth<br>[m]                      | $\delta^{18}\text{O}$ [‰] vs.<br>VSMOW | $\delta\text{D}$ [‰] vs.<br>VSMOW | d-excess [‰] vs.<br>VSMOW | Temperature<br>[°C] |
|--|--|-----------------------------------|---------------------------|---------------------|
| water depth profile taken in August 2012 |  |                                   |                           |                     |
| 0  | -17.89                                 | -134.4                            | 8.7                       | 11.5                |
| 2  | -17.97                                 | -135.9                            | 7.9                       | 11.5                |
| 4  | -17.90                                 | -136.1                            | 7.2                       | 11.5                |
| 6  | -17.85                                 | -134.2                            | 8.6                       | 11.5                |
| 8  | -18.04                                 | -134.4                            | 9.9                       | 10.9                |
| 10                                       | -18.14                                 | -134.3                            | 10.8                      | 10.2                |
| 12                                       | -18.11                                 | -136.9                            | 8.0                       | 9.4                 |
| 14                                       | -18.36                                 | -140.1                            | 6.8                       | 6.9                 |
| 16                                       | -18.21                                 | -138.4                            | 7.2                       | 8.7                 |
| 18                                       | -18.58                                 | -139.3                            | 9.3                       | 6.6                 |
| 20                                       | -18.41                                 | -139.0                            | 8.3                       | 7.5                 |
| 22                                       | -18.02                                 | -135.5                            | 8.6                       | 10.3                |
| 24                                       | -18.50                                 | -139.5                            | 8.5                       | 7.6                 |
| 26                                       | -17.98                                 | -136.0                            | 7.8                       | 10.4                |
| 28                                       | -18.33                                 | -138.9                            | 7.8                       | 7.5                 |
| 30                                       | -18.45                                 | -140.0                            | 7.6                       | 6.7                 |
| 32                                       | -18.61                                 | -141.2                            | 7.7                       | 5.0                 |
| 34                                       | -18.83                                 | -140.8                            | 9.8                       | 4.8                 |
| 37                                       | -18.10                                 | -136.8                            | 7.9                       | 6.6                 |

## **Acknowledgments**

I would like to thank Dr. Hanno Meyer for his dedication, effort and patience and for the opportunity to work on this thesis at Alfred-Wegener-Institute, Potsdam. I also like to thank apl. Prof. Dr. Bernhard Diekmann, and Dr. Boris Biskaborn for the opportunity to participate in the field campaign to Lake Bol'shoe Toko in 2013 and for their support and critical feedback regarding this thesis. Special thanks to Dr. Bernhard Chaplign for his contribution on sampling strategy and field preparation. I like to thank Antje Eulenberg for the explanation and supervision of hydrochemistry analyses. Furthermore, I like to thank all colleagues of the Yakutia/Lake Bol'shoe Toko 2013 Expedition for their help on water sampling and preparation. I'm grateful for the support of my family and Christoph Manthey given at any time.

I gratefully acknowledge the NOAA Air Resources Laboratory (ARL) for the provision of the HYSPLIT transport and dispersion model and READY website (<http://www.ready.noaa.gov>) used in this thesis.

## Selbstständigkeitserklärung

Hiermit versichere ich, dass ich diese Bachelorarbeit selbstständig und nur mit den angegebenen Quellen und Hilfsmitteln angefertigt habe. Alle Stellen der Arbeit, die ich aus diesen Quellen und Hilfsmitteln dem Wortlaut oder dem Sinne nach entnommen habe, sind kenntlich gemacht und im Literaturverzeichnis aufgeführt. Weiterhin versichere ich, dass weder ich noch andere diese Arbeit weder in der vorliegenden noch in einer mehr oder weniger abgewandelten Form als Leistungsnachweise in einer anderen Veranstaltung bereits verwendet haben oder noch verwenden werden.

Die „Richtlinie zur Sicherung guter wissenschaftlicher Praxis für Studierende an der Universität Potsdam (Plagiatsrichtlinie) - Vom 20. Oktober 2010“, im Internet unter <http://uni-potsdam.de/ambek/ambek2011/1/Seite7.pdf>, ist mir bekannt.

---

Ort, Datum

---

Unterschrift